Answers to referee 1

General comments

The paper presents a multiproxy analysis of two short coastal sediments cores collected off Coquimbo, Chile, with the aim to document paleoclimate and paleoceanographicvariability during the Holocene. The data presented is original and valuable to understand the millennial dynamics of the South East Pacific coastal upwelling. Authors analyzed a broad range of geochemical and microfossil indicators which should lead to a robust interpretation. However, substantial work is still needed on the manuscript before being published. I have a few methodological concerns with the chronology and with the way metal concentrations are used, that need to be addressed. The text also requires a lot of work. Except for method sections, the text in general lacks clarity, partly because of inappropriate word choices, and partly because of a lack of focus. The introduction needs to be rewritten since it does not present the context, the research motivation, or the objectives of the work. A proper paleoclimate discussion is missing. Almost no comparison with published results was made and none of the relevant literature on the regional paleoceanography or paleo ENSO is cited. This study deserves to be published but the manuscript requires substantial revision. So far the article is essentially focused on sediment chemistry but lacks depth in the paleoceanographic interpretation and discussion which is the objective. I recommend a more active contribution of co-authors in writing the introduction, discussion and conclusions-

Answer:

The introduction was re-written considering other aspects related to climatic past variability. The last paragraph highlights the objective of our study.

The paleoclimate section (5.4) was rewritten, considering paleoclimatic conditions observed by other authors in the Chilean northern margin. We avoided comparisons with studies conducted over a wide range of time periods which extend beyond the Holocene. Our cores only show records from the mid-Holocene onwards and therefore, we focus our discussion on that time range. We made comparisons with studies conducted near the zone of influence in the northern part of the Southwest Winds so as to prevent the discussion from being unnecessarily long. We included studies that work on our time scale, including: Lamy et al., 1999, 2001, 2010; and Hebbeln et al., 2002. Some of these studies mention the effects of the ENSO in the area, which is the main driver of environmental changes therein. Our objective was not to establish periods of occurrence of these events but to establish changes in productivity and redox conditions, which are obviously subject to climatic and oceanographic forces, such as El Niño. In addition, we included some works by Gutiérrez and Salvatecci conducted in southern Peru, which considers the response of upwelling ecosystems to climatic changes during the last Holocene.

Answers to detailed comments:

Detailed comments:

- The presentation of results in the abstract is unclear:

The text was completely modified from lines 33 to 49.

- The introduction is a lengthy, disorganized list of unfocused information about upwellings in general and sediment proxies. It needs to be entirely rewritten to present the context, the motivation of the research, the scientific questions, the objectives and the scientific strategies chosen to achieve them.

We modified the introduction completely, from lines 56 to 102.

- L132-139: this paragraph on pigments seems unnecessary

We rewrote the section about the study area and we are omitting superfluous information, we deleted the paragraph between lines 132 and 139.

- L145: the words "relevance" and "relevant" are repeatedly used in an inappropriate way throughout the manuscript.

We modified all lines and replaced the word for other more appropriate terms, except in lines 555 and 706.

- L167-172: unprecise

- L176-178: the fact that two sediments cores were analyzed and their location should be mentioned in the introduction

We added extra information at the end of the introduction; see lines 118 to 122. We provided further explanation about our point at the end of the study area section, lines 161-167.

- *Trace metal concentrations:*

The normalization of Me concentrations using Al does not seem justified to me. The analytic technique used here (ICPMS analyses of dissolved samples) yields quantitative and absolute concentration values thanks to the standards used. As far as I know, uncertainties related to machine variability and matrix effects are not an issue with this technique as it would be with laser ablation technique. In addition, Al does not have a conservative behavior as mentioned: figure 10 shows on the contrary a substantial increase of Al concentration through the Holocene. Normalizing systematically with this element may actually produce biased interpretations.

Al normalization is extensively used in geochemical studies. The conservative elements are not affected by chemical or biological processes, but affected by physical; it does not mean that their concentration does not change. It is important to estimate the authigenic enrichment of the elements. This process occurs in situ and in some way depends on the metal fluxes, but the environmental conditions determine the enrichment of these elements, see Calvert and Pedersen (2007), Tribovillard et al., (2006), Böning et al. (2004, 2005, 2009) among others. This allows discriminating between enrichment and terrestrial input; therefore the variability of Al can imply variability in some elements with greater terrestrial impacts than other processes. Some elements can be used as indicators of terrigenous inputs and their variability can display whether the variability in sedimentary records accounts for contributions from land or for changes in primary productivity or redox conditions. Therefore, each element must be normalized to Al or Ti, which is also useful to remove the effect of variability produced by changes in grain size. There is some concern about the use of Al and Ti for this purpose. However, caution must be used when using Al or Ti for the interpretation of metal distributions.

The normalization is not related to ICPMs technique. We do not use laser ablation.

I recommend to use the accumulation rate from the age model and absolute Me concentration to calculate metal fluxes to the sediment.

The accumulation rate could be a choice but is highly influenced by the age model used. Therefore, a better choice is to use the metal/Al ratio instead of the accumulation rate to establish authigenic enrichment. Accumulation does not depend on the fluxes, it depends on other on site factors that are useful to decipher the redox conditions at bottoms.

Since Al has mainly a continental origin, ratios with Al is informative for elements whose flux is related to productivity to discuss relative contribution of marine vs terrestrial contributions in the sediment.

All elements have an earth crust origin. While some elements follow different cycles, like nutrient type elements, they are incorporated into marine organism and deposited on the bottom when primary production settles down. After that, the elements follow other mechanism that allow for their enrichment, depending on their affinity to sulfides, for example. Therefore the normalization with Al is appropriate.

Finally, the usefulness of the enrichment factors is not obvious. Figure 9 is barely discussed. In addition, I wonder if wetland sediments are really representative of crustal metal concentrations since they also contain organic matter.

We decided to add a table (table 5) with the most relevant information to indicate that the variations in metals during periods of higher/lower productivity (based on opal accumulations rate) are due to authigenic enrichment, which in turn is a consequence of changes in redox conditions and not variations of continental inputs**.**

- Geochronology
L248: Calpal2007_HULU calibration curve is an odd choice for radiocarbon calibration.

We made corrections in the text; we use Clam2.2 program.

It is also inconsistent with L255 in which Marine13 is mentioned (which is the correct calibration curve to use). There is a couple of issues with the regional radiocarbon reservoir age used for calibration. First, the method to calculate it is not correct. 14C reservoir age should be calculated in the 14C age scale, not in the calendar scale as it was done here. dR is the difference between the marine sample 14C age and the 14C

age that corresponds to the absolute age (here obtained from the 210Pb model) using the Marine13 curve. See Southon et al. (1995) for details on the technique. The dR value obtained here is larger than any dR values obtained previously on the Chilean coast Authors should read and use Ortlieb et al., 2011; Carré et al., 2016; and Merino-Campos et al., 2018. The latter reference presents 37 prebomb dR values all along the Chilean coast measured with a reliable technique. Using a value from this publication would be more reliable. The first 2 references show changes in dR values through the Holocene that should also be discussed. Finally, instead of BC/AD, ages should all be presented in the BP scale as it is usual in paleoceanography for Holocene studies.

We added an explanation in the text. We think upwelling waters are affecting the age of foraminifers in our cores sites; other records at deeper areas have also used a DR ~ 400 years (De Pol-Holz, 2007). The samples of Carré and Meirno-Campos are submareal species that live at shallows depths (<30 m), not highly affected by the upwelling. We resorted to the method used by Sabatier et al., (2010) and we added a table for informational purposes (table 3). Our estimations considers two pre-bomb data at 5 and 10 cm depth in the sediment cores from Guanaqueros and Tongoy bays; the ages from 210Pbxs correspond 499 and 448 years BP (Reimier et al., 2013) and were compared with radiocarbon ages from foraminifers at the same depths. In both cases we obtain similar results, therefore we decided to maintain the original age models, considering 441 years as a local reservoir. These values should correspond to the direct effect of old upwelled waters in agreement with oceanographic conditions on the sampling stations.

We changed all Cal AD/BC to Cal BP ages.

Discussion:

L505-L514: unclear
L521-L536: the discussion about d13C values is unclear, in part because there seem to be a confusion between Total organic carbon(TOC) in the water column and suspended particulate organic Matter (SPM). Is it possible that the difference between d13C values in the water and in the sediment are due to the difference between TOC and SPM? A preferential degradation of 13C enriched particles is mentioned (L528-529): could you support this with a reference?

L563-L568: the discussion about K is not very convincing. A reference about the detritic origin of K is needed. Ca could also have a detritic origin so close to the shoreline. Al, Fe are also clear terrestrial input indicators. Why not discuss them together?

We added the reference and Ca is normally used as an indicator of marine productivity versus K, which is a major element that has no implications on marine productivity. Fe is more complicated due to its double origin. In all cases, we attempted to use the best proxy in order to interpret each process.

L602-L606: references needed

Section 5.3 should be shortened. It is somewhat redundant with other discussion sections and the result section.
- Climatic interpretations

We rewrote this section completely.

This section lacks in-depth discussion. The results here should be compared to published results to understand how they contribute, support or contradict existing hypothesis about millenial oceanographic variability in Chile.
L720-L723: "past changes are analogue with the present meridional displacement of the ITCZ and the SPCH". This should not be taken as a fact. It is only a hypothesis used as an interpretation model.
L744-L747: this part is unclear and sounds contradictory (a poleward shift of **SWWshould not promote humid conditions in central Chile). In addition, this is a model result.**

Why not compare with existing paleoenvironmental and paleoceanographic data?

There is a series of sediment cores that document past oceanographic conditions in the Peru-Chile upwelling system during the Holocene. This includes Lamy et al (1999, 2001, 2002, 2010), Kim et al. (2002), Hebbeln et al. (2002), Rein et al. (2005), Salvatecci et al. (2014, 2016). On a regional scale, the data presented here confirm a La Niña-like situation in the early to mid-Holocene, which is in agreement with previous datasets including Koutavas et al. (2002), Fontugne et al. (2004), Conroy et al. (2008); Carré et al. (2012), and model experiments such as Brown et al. (2008); Braconnot et al. (2012), Luan et al. (2015). This list is clearly not exhaustive.

The first version of this manuscript considered the information of studies by Lamy, Hebbeln, Salvatteci. We added others from the list suggested, but focused on the range of time that covered our study and on Chile's central margin. Some studies about southern Peru were also cited. We re-wrote the paleoclimate section and considered the main studies focused from mid-Holocene in the region, identifying the main environmental conditions prevailing during the maximum periods of primary productivity.

The influence of ENSO variability needs obviously to be discussed. It is here briefly mentioned in the text, appears in the key words, but there is no discussion. Data on past ENSO activity do exist (Koutavas et al., 2006; Cobb et al., 2013; Carré et al., 2014) and they need to be included in the discussion if the role of ENSO in the presented data is to be evaluated.

We discussed some details about ENSO. Our study is not focused on the ENSO variability, but on changes in primary productivity and redox conditions.

Figure 2: what about st14? Font on Y scale too small Figure 3: SPM is not the same as TOC Figure 5: it is not clear which curve is grain size and which is susceptibility

We have no oxygen data for st14 and we made the corrections in the figures.

Figure 6: Al and Fe are both related to terrestrial input. What information does Fe/Al provide?

It could show enrichment of Fe by oxidation.

Figure 9: This figure is not commented in the text. EF calculation does not seem useful.

We changed it for a more informative and brief table.

Answers to referee 2

The authors present a large range of biogeochemical and microfossil proxies and the results are worth to be published. However, I agree with referee #1 that the discussion of the results is not sufficient and needs substantial alteration, more in-depth interpretation of the own data as well as comparison to relevant literature.

Initially, we used several references for the study area. To favor comparable results and since most works extend further back from the Holocene, we avoided using research that went beyond the period of time during which we did our work.
We also tried to focus on the area of study. Much work has been carried out far north or far south, with different responses to atmospheric and oceanographic forcing. These results are not comparable since our objective was to identify changes in productivity and changes in redox conditions in the past. While our findings complement the main results of other studies in the Chilean continental margin, they also provide information on the possible effects on atmospheric-oceanographic changes in one of the most important upwelling areas of the Chilean continental margin.
We modified the introduction, the last part of the section about the study area and the last part of the discussion regarding paleoclimatic interpretations, and we used several of the references you suggested.
. We believe this improves the discussion of our findings.

The Discussion is too short especially in comparison to the methods section. There is actually room for more detailed interpretations, for example the Nitrogen isotopes
are not explained or discussed at all. The connections between sentences and paragraphs are often weak or confusing, there is some refinement needed and the reader must be led more through the text, especially the discussion. As the manuscript reads now it appears as you randomly choose some results to discuss one after the other. For example see paragraphs starting in lines 521 and 537. To further strengthen the discussion add more comparisons to local studies such as (Contreras et al., 2007; Díaz-Ochoa et al., 2010; Fukuda et al., 2013; Mohtadi et al., 2008; Ortega et al., 2012).

The discussion in point 5.1 refers to the biogenic versus the terrigenous contributions. First, the organic component has been discussed when we talk about TOC and stable isotopes; then the inorganic, when we comment on the susceptibility and magnetic and metals.
A paragraph has been included regarding the implications of the changes in the 15N distribution and we have added citations, such as DePol-Holz. Contreras has not been considered because his work is focused on superficial sediments and temporal variation of 15N. The study by Mohtadi et al 2008 does not highlight any results for the mid-Holocene; their core's data dates back 6 Ka and our study could be comparable only in some parts of their charts. It could be compared with our study only in a few points of its graphs. The core used off the Coquimbo area corresponds to depths in the slope under the influence of Intermediate Antarctic Water, as this study is focused on studying the changes of this water body after the Last Glacial Maximum. We included Ortega as a work submitted since the manuscript is forthcoming. However, this manuscript is based on the analysis of a short core of the Tongoy Bay. . In the case of Díaz-Ochoa, the work focuses on the last 200 years, the implications of which do not

match our records. Additionally, the oceanographic dynamics in Mejillones are considerably different from those in Coquimbo.

Through the whole manuscript the authors refer to suboxic/anoxic conditions, however, the values given for the water station 16 seems to be well above the suboxic value of <0.2 ml/L. For station 1 it's really hard to distinguish if the values may be lower sometimes. I think the value ranges for oxic/suboxic/anoxic need to be given in the introduction. Also, while water values are presented the oxygen levels discussed refer to the sediment which needs to be made much clearer. Just because you have low oxygen in the water column this does not necessarily make the underlying sediments anoxic.

In the present conditions, bottom waters are normally suboxic. Therefore, in our sedimentary records the enrichment of metals like U, Re and Mo decrease dramatically. When we speak of anoxia, we are referring to periods in the past for which there are no oxygen records, but it is deduced from the distribution of proxies like U, Re and Mo, which point to a very low content of oxygen and even sulfides, suggested by a large enrichment of Cd and Mo. Strictly speaking, all the sediments are anoxic; the penetration of oxygen is only a few mm when the bottom waters are suboxic. In our case, the high deposition of organic material generates seasonal conditions of anoxia on the sediments due to high consumption during its degradation. Then these sediments are under the effect of anoxic conditions which seem to prevail during the mid-Holocene.

Add a discussion of the nitrogen isotope data. And compare to previous studies, such as (De Pol-Holz et al., 2006; 2007; Verleye et al., 2013).

We added a paragraph considering the works of De Pol-Holz and others that help establish the effect of the OMZ and upwelling on our site, thereby complementing our interpretations of metal distribution**.** Lines 537 to 551. No interpretations on nitrate reduction variability could be done since our core covers from the mid-Holocene onwards and because no major changes in 15N are expected during this period.

General remarks:
The figures are often not focused, the labels are too small, and in figure 10 the age should be plotted on the y-axis as in the other figures.

We corrected the figures, except the figure on moisture pollen which displays better horizontally.

I would like to see a more comprehensive conclusion, so far it's more a summary. Suggestion: try to reduce information in methods and results section. Is the exact.

We modified the conclusions.

Munsell chart colour really needed?
Is a good guide for establishing the general composition of the sediments

For example get rid of Line 181 to 183.
These lines briefly explain how the cores were processed.

Specific remarks:

Figure 1: Please add the surface circulation for the area.

We added an outline of bay circulation based on studies available; some patterns are under study and yet to be defined.

This is relevant to understand the arguments raised.

Figure 2: unsharp and colors are hard to distinguish, this needs revision, I suggest to use a color range that is more appropriate to highlight the DO values of the low end of the scale more. Numbers in this plot need to be larger as well.

We made the corrections and chose the best colors allowed by the Matlab program.

Figure 5: I think the accumulation rates for TOC should be given here instead of just (%), further please add the core number directly behind a.) and b.) in the figure.

The organic carbon accumulation was included in the figures 5a and 5b and in the text, but the sedimentation rate does not change much, so to do a calculation with a relatively constant number does not contribute mostly to the results.

Figure 10: I suggest to also put the Age on the Y-axis here as in all the other figures.

Line 35 – add "The" before Coquimbo

Line 78 to 83: rephrase, you cannot refer to "these boundary current ecosystems" in one sentence and then explain it afterwards.

Line 131-132: maximum Chl a concentrations of ...

Line 209-216: remove this paragraph, the section is already long and you only list the following chapters here.

Line 218: change the comma to a dot.

Line 384- 390. This was a bit confusing as a southern and northern area are introduced, but both cores studied are in the southern area?

Line 720: "Past environmental changes are analogue..." please specify these changes clearly here.

Line 724: "in this regard", it's not clear what you are referring to

Line 726: Studies based on pollen records ... There is a citation missing here!

Line 747-51: rephrase, improve the connection to the sentence before by first saying that you see indications of higher continental inputs due to increased rainfall, than which of your data shows this and which other studies support this observation. I further suggest to split this sentence in two.

Line 759: rephrase "peak drying"

Most of these lines were modified. We checked grammar mistakes and we modified several lines and paragraphs in order to answer to the comments by both referees.

This marked-up version include all suggestions. Main changes were highlighted.

Reconstructing past variations in environmental conditions and paleoproductivity over the last ~8000 years off Central Chile (30° S)

Práxedes Muñoz[1,2], Lorena Rebolledo[3,4], Laurent Dezileau[5], Antonio Maldonado[2], Christoph Mayr[6,7], Paola Cárdenas[4,8], Carina B. Lange[4,9,10], Katherine Lalangui[9], Gloria Sanchez[11], Marco Salamanca[9], Karen Araya[1,5], Ignacio Jara[2], Gabriel Vargas[12], Marcel Ramos[1,2].

[1]Departamento de Biología Marina, Universidad Católica del Norte, Larrondo 1281, Coquimbo, Chile.
[2]Centro de Estudios Avanzados en Zonas Áridas (CEAZA), Coquimbo-La Serena, Chile.
[3]Departamento Científico, Instituto Antártico Chileno, Punta Arenas, Chile.
[4]Centro FONDAP de Investigación Dinámica de Ecosistemas Marinos de Altas Latitudes (IDEAL), Universidad Austral de Chile, Campus Isla Teja, Valdivia, Chile.
[5]Laboratoire Géosciences Montpellier (GM), Université de Montpellier, 34095 Montpellier Cedex 05, France.
[6]Institut für Geographie, FAU Erlangen-Nürnberg, 91058 Erlangen, Germany.
[7]Department of Earth and Environmental Sciences & GeoBio-Center, LMU Munich, 80333 Munich.
[8]Programa Magister en Oceanografía, Universidad de Concepción, casilla 160C, Concepción, Chile.
[9]Departamento de Oceanografía, Facultad de Ciencias Naturales y Oceanográficas, Universidad de Concepción, Casilla 160C, Concepción, Chile.
[10]Centro de Investigación Oceanográfica COPAS Sur-Austral, Universidad de Concepción, Casilla 160C, Concepción, Chile.
[11]Universidad de Magallanes, Punta Arenas, Chile.
[12]Departamento de Geología, Universidad de Chile, Santiago, Chile.

Correspondence: Práxedes Muñoz (praxedes@ucn.cl)

Abstract

The Coquimbo (30°S) region, in the North-central Chilean Coast, is characterized by relative dry summers and a short rainfall period during winter months. The wet-winter climate results from the interactions between the Southern Westerly Winds and the South Pacific Anticyclone (SPA). Interdecadal climate trends are mostly associated with El Niño-Southern Oscillation (ENSO), which produces high variability in precipitation. With the aim of establishing past variations of the main oceanographic and climatic features in the Central Chilean coast, we analyze recent sedimentary records of a transitional semi-arid ecosystem susceptible to environmental forcing conditions. Sediment cores were retrieved in two bays, Guanaqueros and Tongoy (29−30°S), for geochemical analyses including: sensitive redox trace elements, biogenic opal, total organic carbon (TOC), diatoms, stable isotopes of organic carbon and nitrogen. Three main periods of increased productivity were established: (1) > cal BP 6500, (2) cal BP 2100 – cal BP 4600 and (3) during recent time (CE 2015) – cal BP ~260. The first period was conspicuously high during the main dry phase concomitant with high fluxes of organic compounds to the bottom and suboxic-anoxic conditions in the sediments. This period reached a maximum at cal BP ~6500, at the time of the maximum Holocene transgression reported for the zone (~ cal BP 6380), followed by a continuous increase in moisture levels, low primary productivity and a more oxygenated environment towards the present, being remarkably stronger in the last 2000 years. We suggest that this might be associated with greater El Niño frequencies or similar conditions that increase precipitation, concomitantly with the introduction of oxygenated waters to coastal zones by the propagation of equatorial origin waves.

Keywords: paleoproductivity, paleoredox, trace metals, diatoms, opal, organic carbon, Coquimbo, SE-Pacific

1. Introduction

The northern-central Chilean continental margin (18−30°S) has distinct zones of intense upwelling highly influenced by topographic features (Figueroa and Moffat, 2000). As a result, high primary production (0.5-9.3 g C m^{-2} d^{-1}) are developed off Iquique (21°S), Antofagasta (23°S) and Coquimbo (30°S) (González et al., 1998; Daneri et al., 2000, Thomas et al., 2001). This productivity takes place close to the coast above the narrow continental shelf, allowing the development of important fisheries and accounting for up to 40% of total annual catches (Escribano et al., 2004 and references therein).

This high productivity maintains a zone of low dissolved oxygen content along the Chilean margin, reinforcing the oxygen minimum zone (OMZ) that develops along the North and South Pacific Ocean, where their intensity, thickness, and temporal stability vary as a function of latitude (Helly and Levin, 2004, Ulloa et al., 2012). To the north (e.g. 21°S) and off Peru, the OMZ occurs permanently, can extend into the euphotic zone and, in the case of northern Chile and southern Peru, shows no significant interface with the benthic environment due to the presence of a narrow continental shelf (Helly and Levin, 2004).

Past changes in the productivity and oxygenation of bottom waters at different timescales have been evidenced in the SE Pacific through sedimentary records that cover from the Last Glacial Maximum (cal BP 22,000 −18,000) to the present. Different climate-ocean drivers have been proposed to account for these changes. For instance, latitudinal movements of the Southern Westerlies Winds (SWW) and the Antarctic Circumpolar Current (ACC) have been suggested as potential mechanisms (Hebbeln et al., 2002; Lamy et al., 2001; 2002; 2010). In addition, changes in the intensity and position of the Southeast Pacific Subtropical Anticyclone (SPSA) from seasonal, to interdecadal timescale have effects on wind stress and water mass circulation (Ancapichún and Garcés-Vargas, 2015), and therefore past variability in the SPSA has been used to explain changes in paleoceanographic features of the SE Pacific such as the intensity of upwelling, and circulation patterns responsible for the nutrient supply (Marchant et al., 1999; Hebbeln et al., 2002; Dezileau et al., 2004; Romero et al., 2006; Mohtadi et al., 2008; Gutiérrez et al., 2009; Saavedra-Pellitero et al., 2011; Muñoz et al., 2012). Past climate-upwelling fluctuations at millennial timescales has also been linked to the austral insolation, which influence Antarctic sea ice extent and the Hadley cell, this latter an important forcing to the latitudinal cycle of the ITCZ (Intertropical

Convergence Zone; Kaiser et al., 2008 and reference there in). This variability produces humid and arid conditions along the SE Pacific where the intensity of wind has a key role for the upwelling and hence productivity. On top of all this, an important driver of modern ocean-atmosphere conditions in the South East Pacific is the El Nino/Southern Oscillation (ENSO), which has a major impact on modern marine productivity (Escribano et al., 2002). Paleo-ENSO reconstructions indicate attenuated ENSO events before the mid-Holocene (last 5000 years) and increasing from this period towards the present (Marchant et al., 1999; Koutavas et al., 2006; Vargas et al., 2006), consistent with paleoceanographic and paleoclimate interpretations (Rodbell et al., 1999; Rein et al., 2005). Heavy rainfall episodes in the south East Pacific normally occur during strong El Niño conditions (Montecinos and Aceituno, 2003), increasing the river flux and producing flood debris (Garreaud and Rutllant, 1996). These episodes have been recorded in sedimentary records off northern Chile and southern Peru, establishing a teleconnection which has operated since the mid-Holocene, and identifying the modern manifestation of El Niño starting at ~5300 − 5500 cal BP (Vargas et al., 2006).

The effect of climate variations on primary productivity and biogeochemical cycles could have different responses. For instance, the increase in land-sea thermal contrast in North-Central Chile enhances upwelling and with it, exported production (Vargas et al., 2007). Other evidence, however, suggest that the intrusion of warmer oligotrophic water reduce primary productivity, as observed during the 97-98 ENSO event (Iriarte and Gozález, 2004). Furthermore, in South central Chile (36°S) the oxygenation of bottoms was clearly detected during the 97-98 El Niño event, changing the geochemical conditions of surface sediments and macrofauna composition. These disturbances may extend considerably to the south, with implications persistent for many years and impact the sedimentary records of several proxies (Sellanes et al., 2007; Gutiérrez et al., 2006). Our work focuses on the past variations of the environmental conditions and marine productivity in sedimentary records from a transitional semi-arid ecosystem of Central Chilean coast (30°S), an area highly susceptible to oceanographic and climatic forcing. The study area (Fig. 1) provides an adequate platform to observe environmental variability at different time scales. We were able to identify wet/dry intervals, periods with high/low primary production, and changes in redox conditions at bottoms through inorganic (trace metals) and organic proxies.

2. Study area

The Coquimbo area (29-30°S), in the southern limit of the northern-central Chilean continental margin, constitutes a border area between the most arid zones of northern Chile (Atacama Desert) and the more mesic Mediterranean climate of central Chile (Montecinos et al., 2016). Here, the shelf is narrow and several small bays trace the coast line.

The Tongoy and Guanaqueros bays are located at the southern edge of a broad embayment between small islands in the north (29°S; Choros, Damas and Chañaral) and Lengua de Vaca Point in the south (30°S) (Fig. 1), protected from predominant southerly winds. Tongoy Bay is a narrow marine basin (10 km at its maximum width) with a maximum depth of ~100 m. To the northeast lies Guanaqueros Bay, a smaller and shallower basin. Favorable winds throughout the year promote an important upwelling center at Lengua de Vaca Point, developing high biomass along a narrow coastal area (Moraga-Opazo et al., 2011), and reaching maximum concentrations of ~20 mg m^{-3} (Torres and Ampuero, 2009). At the shallow waters of Tongoy Bay, the high primary productivity results in high TOC in the water column allowing the deposition of fine material on the bottom; TOC increases concurrently with the periods of low oxygen conditions (Fig. 3; Muñoz et al., unpublished data). Recent oceanographic studies indicate that the low dissolved oxygen water intrusions from the shelf (Fig. 2) seems to be related to sea level decreases resulting from local wind annual cycles at a regional meso-scale (Gallardo et al., 2017). The spatial and temporal variability of these processes are still under study.

Sedimentological studies are scarce in the northern-central Chilean shelf. A few technical reports indicate that sediments between 27°S and 30°S are composed of very fine sand and silt with relatively low organic carbon content (<3 and ~5%), except at very limited coastal areas where organic material accounts for around ~16% (Muñoz, unpublished data; FIP2005-61 Report, www.fip.cl). Coastal weathering is the main source of continental input due to scarce river flows and little rainfall in the zone (0.5 to ~80 mm yr^{-1}; Montecinos et al., 2016, Fig.1). Freshwater discharges are represented by creeks, which receive the drainage of the coastal range forming wetland areas in the coast and even small estuaries, as Pachingo located south of Tongoy (Fig. 1). These basins cover ~300 and 487 km^2, respectively. The water volume in the estuaries is maintained by the influx of seawater mixed with groundwater supply. No surface flux to the sea is observed. Therefore, freshwater discharge occurs only during high rainfall periods in the coastal zone (DGA, 2011), which normally takes place during El Niño years when higher runoff has been recorded in the area during austral winter time (Valle-Levinson et al., 2000; Garreaud et al., 2009). In this scenario marine sediments are often highly influenced by primary production in the water column, and therefore sedimentary records can reveal past variability in primary production and the oceanographic conditions over the shelf, which ultimately respond to major atmospheric patterns.

3. Materials and methods

3.1. Sampling

Sediment cores were retrieved from two bays in the Coquimbo region: Bahía Guanaqueros (core BGGC5; 30°09' S, 71°26' W; 89 m water depth) and Bahía Tongoy (core BTGC8; 30°14' S, 71°36' W; 85 m water depth) (Fig. 1.), using a gravity corer (KC-Denmark) in May 2015, on board the L/C Stella Maris II owned by the Universidad Católica del Norte. The length of the cores was 126 cm for BGGC5 and 98 cm for BTGC8. Both cores were cut along the main axis and a general visual characterization was done. Different textures and color layers were identified using the Munsell color chart.

Subsequently, the cores were sliced into 1-cm sections and subsamples were separated for grain size measurements, magnetic susceptibility, trace elements, biogenic opal, C and N stable isotope signatures ($\delta^{13}C$, $\delta^{15}N$), and TOC analyses. The samples were first kept frozen (–20° C) and then freeze-dried before laboratory analyses.

The magnetic signal indicates the concentrations and compositions of magnetic minerals and is usually used combined with others detrital proxies such as grain size to establish changes in sedimentary processes closely controlled by climatic conditions. We considered redox trace elements measurements that respond to local hypoxia (U, Mo and Re) as well as nutrient-type elements, which follow the organic fluxes to the sediments (Ba, Ni Cu, P). Additionally, we measured Fe and Mn which play a key role in adsorption-desorption and scavenging processes of dissolved elements in the bottom water and sediments. We also measured Ca, K and Pb used to assess terrigenous inputs by coastal erosion, weathering and eolian transport, which is also true for Fe and Mn. Ca accumulation within the sediments depends, in turn, on the carbonate productivity and dissolution, which has been used as a paleoproductivity proxy (Paytan, 2008; Govin et al., 2012). We use Al as a normalizing parameter for enrichment/depletion of elements due to its conservative behavior. The crustal contribution and the elements are presented as metal/Al ratios. The authigenic enrichment factor of elements was estimated according to: EF = $(Me/Al)_{sample}$ / $(Me/Al)_{detrital}$; where $(Me/Al)_{sample}$ is the bulk sample metal (Me) concentration normalized to Al content and the denomination “detrital” indicates a lithogenic background (Böhning et al., 2009). Detrital concentrations ($[Me]_{detrital}$ and $[Al]_{detrital}$) were established considering the local TM abundance, which is more accurate than using mean Earth crust values (Van der Weijden, 2002). We used the average of element concentrations at the surface sediments (0−3 cm) of Pachingo wetland (Table 1).

Diatoms and siliceous microfossils were identified and counted. Diatoms assemblages along with biogenic opal content constitute our proxies of siliceous export production. Pollen grains were also identified and counted, and used to identify wet and dry environmental conditions based on the climate relationship of the main vegetation formation in north-central Chile. TOC and stable isotopes of organic matter were used to identify the variability of organic fluxes to the bottom and establish biogeocheemical changes in the organic matter remineralization.

3.2. Geochronology (^{210}Pb and ^{14}C)

^{210}Pb activities were quantified through alpha spectrometry of its daughter ^{210}Po in secular equilibrium with ^{210}Pb, using ^{209}Po as a yield tracer (Flynn, 1968). The chemical procedure considered a total digestion of the sediment samples and then autoplated onto silver disks at ~75°C for 3 three hours in the presence of ascorbic acid. The ^{210}Po activity was counted in a CANBERRA QUAD alpha spectrometer, model 7404, until the desired counting statistics was achieved (4−10% 1σ errors) in the Chemical Oceanography Laboratory of Universidad de Concepción. ^{210}Po activity –assumed to be in secular equilibrium with ^{210}Pb– was calculated using the ratio between natural radionuclide and the tracer, which is multiplied by the activity of the tracer at the time of plating. The period elapsed between plating and counting produces ^{210}Po decay (half-life: 138 days) and between sampling and plating ^{210}Pb decay (half-life: 22.3 yr); counting was corrected to these elapsed times even when there was a short time period between the collection date and the time of sample analysis (less than one year). Ages were estimated using the inventories of the activities in excess ($^{210}Pb_{xs}$, unsupported), based on the Constant Rate of Supply Model (CRS, Appleby and Oldfield, 1978). Unsupported activities were determined as the difference between ^{210}Pb and ^{226}Ra activities measured in some sediment column intervals. ^{226}Ra was measured with a gamma spectrometry at the Laboratoire Géosciences of the Université de Montpellier (France). Standard deviations (SD) of the ^{210}Pb inventories were estimated propagating counting uncertainties (Bevington and Robinson, 1992) (Table S1, supplementary data). Radiocarbon measurements were performed on a mix of planktonic foraminifera species in core BGGC5 whereas the benthic foraminifera species *Bolivina plicata* was selected for core BTGC8 (Table 2). Freeze-dried sediment was washed over a 63 µm mesh-size sieve and dried after washing at 50°C. At least 2 mg of mixed planktonic foraminifera were picked from the 125–250 µm fraction. The samples were submitted to the National Ocean Sciences AMS Facility (NOSAMS) of the Woods Hole Oceanographic Institution (WHOI). The Fraction Modern (Fm) was corrected by the $\delta^{13}C$ value, and ages were calculated using 5568 (yrs) as the half-life of radiocarbon. The time scale was obtained according to the best fit of ages obtained from $^{210}Pb_{xs}$ and ^{14}C (Fig. 4), using the CLAM 2.2 software and Marine curve 13C (Reimer et al., 2013) considering a reservoir deviation from the global mean reservoir age (DR) of 441 ± 35 years, established according Sabatier et al. (2010). This was estimated subtracting the age value corresponding at the historical dates 1828 AD and 1908 AD (499 ± 24 and 448 ± 23 ^{14}C yr, respectively, Reimer et al., 2013) from the apparent ^{14}C age of foraminifers measured at depths of 5 and 10 cm for cores BTGC8 and BGGC5, respectively (Sabatier et al., 2010; Table 3).

3.3. Geophysical characterization

Magnetic susceptibility ($SIx10^{-8}$) was measured with a Bartington Susceptibility Meter MS2E in the Sedimentology Laboratory at Centro Eula, Universidad de Concepción. Mean values from three measurements were calculated for each sample.

Grain size was determined using a Mastersizer 2000 laser particle analyzer, coupled to a Hydro 2000–G Malvern in the Sedimentology Laboratory of Universidad de Chile. Skewness, sorting and kurtosis were evaluated using the GRADISTAT statistical software (Blott and Pye, 2001), which includes all particle size spectra.

3.4. Trace elements analysis

Trace element analyses were performed by ICP-MS (Inductively Coupled Plasma-Mass Spectrometry) and carried out at Université de Montpellier 2, France (OSU OREME/AETE regional facilities), using an Agilent 7700x. About 50 mg of samples and geochemical reference materials (UBN, BEN and MAG1) were dissolved twice through the conventional digestion method using a concentrated HF-HNO_3-$HClO_4$ mix (1:1:0.1) in Savillex screw-top Teflon beakers at 120°C, on a hot plate during 48h. Following digestion, the samples were subjected to three evaporation steps in order to remove fluorine. Shortly before analysis, samples were dissolved in 2 ml of concentrated HNO_3 and transferred to 20 ml polypropylene bottles. Final sample preparation was undertaken by dilution with ultrapure water to a sample-solution weight ratio of 1: 4000-5000 and the addition of a known weight of internal standard solution consisting of 1 ppb of In and Bi. Internal standardization used ultra-pure solution enriched in In and Bi, both elements whose natural abundances in geological samples do not contribute significantly to the added internal standard. This is used to deconvolve mass-dependent sensitivity variations of both matrix and instrumental origin, occurring during the course of an analytical session.

Sample introduction uses a peristaltic pump, a micro-nebulizer and a cooled double-pass Scott type spray chamber. The uptake time (typically 45 s) is set to facilitate stable analyte signals prior to a 120 seconds analysis for each sample. Elements with an atomic mass lower than 80 were analyzed in collision mode using He; heavier elements were analyzed in no-gas mode. A wash out procedure consisting of 60 seconds with HNO_3 10% and 120 seconds with 2% HNO_3 has been found appropriate to achieve instrument blank level. The total time for analysis of a single sample solution is *c.* 3 minutes. Mean concentrations for the analyzed samples were determined by external calibrations prepared daily from multi- and mono-elemental solutions, with concentrations in the range of 0.05−10 ppb for trace elements and of 1−10 ppm for major elements (Ca, K). Polyatomic interferences were controlled by running the machine at an oxide production level <1%. Typical analytical precisions attained by this technique are generally between 1% and 3%, relative standard deviation. Accuracy has been assessed with an analysis of international reference materials and results show agreement generally better than ±5% with reference values.

3.5. TOC and stable isotopes

TOC and stable isotope ($\delta^{15}N$ and $\delta^{13}C$) analyses were performed at the Institut für Geographie, Friedrich Alexander Universität (FAU) Erlangen-Nürnberg, Germany. Dry material was placed into tin and silver capsules for N and C analyses respectively, and combusted at 1060° C in a continuous helium flow in an elemental analyzer (NC2500, Carlo Erba), in the presence of chromium oxide and silvered cobalt oxide. The resulting gases, were passed over copper wires at 650° C to reduce nitrogen and excess oxygen.

Thereafter, water vapor was trapped with $Mg(ClO_4)_2$ and the remaining gases (N_2 and CO_2) were separated in a gas chromatography column at 45° C. N_2 and CO_2 were passed successively via a ConFloII interface into the isotope-ratio-mass spectrometer (Delta Plus, Thermo-Finnigan) and isotopically analyzed. Carbon and nitrogen contents were determined from the peak-area-versus-sample-weight ratio of each individual sample and calibrated with the elemental standards cyclohexanone-2,4-dinitrophenylhydrazone ($C_{12}H_{14}N_4O_4$) and atropine ($C_{17}H_{23}NO_3$) (Thermo Quest). A laboratory-internal organic standard (Peptone) with known isotopic composition was used for final isotopic calibrations. Stable isotope ratios are reported in the δ notation as the deviation relative to international standards (Vienna Pee Dee Belemnite for $\delta^{13}C$ and atmospheric N_2 for $\delta^{15}N$), so $\delta^{13}C$ or $\delta^{15}N = [(R\ sample/R\ standard) - 1] \times 10^3$, where R is $^{13}C/^{12}C$ or $^{15}N/^{14}N$, respectively. Typical precision of the analyses was ±0.1‰ for $\delta^{15}N$ and $\delta^{13}C$.

3.6. Biogenic opal

Biogenic opal was estimated following the procedure described by Mortlock and Froelich (1989) with a slight modification, which consists in extracting 50 mg of sediment with 1 M NaOH (instead of 2 M Na_2CO_3) at 85°C for 5 hours. Extraction and analysis by molybdate-blue spectrophotometry (Hansen and Koroleff, 1999) were conducted at the laboratories of Marine Organic Geochemistry and Paleoceanography, University of Concepción, Chile. Values are expressed as biogenic opal by multiplying the Si (%) by 2.4 (Mortlock and Froelich, 1989). Analytical precision was ± 0.5%. Accumulation rates were determined based on sediment mass accumulation rates and amount of opal at each core section in %.

3.7. Diatoms and siliceous microfossils

Smear slides for qualitative abundances of siliceous microfossils were carried out every centimeter following the Ocean Drilling Program (ODP) protocol described by Mazzullo et al. (1988.) To determine the quantitative abundance of siliceous microfossils (diatoms, silicoflagellates, sponge spicules, crysophyts and phytoliths), ~ 0.5 g of freeze-dried sediment was treated according to Schrader and Gersonde (1978). Samples were chosen every ~4, 8 and 12 cm for BGGC5 and at an average of 6 cm for BTGC8. Permanent slides were prepared by placing a defined sample volume (0.2 ml) onto microscope slides that were then air-dried and mounted with Naphrax mounting medium (refraction index

=1.3). Siliceous microfossils were identified and counted under an Olympus CX31 microscope with phase contrast. 1/5 of the slides were counted at 400X for siliceous microfossils and one transect at 1000x was counted for *Chaetoceros* resting spores. Two slides per sample were counted; the estimated counting error was 15%. Total diatom abundances are given in valves g^{-1} of dry sediments.

3.8. Pollen

Sample preparation for pollen analysis was conducted following the standard methodology for sediment samples (Faegri and Iversen, 1989), which includes deflocculating with 10% KOH, carbonate dissolution with a 5% HCl treatment, silica dissolution with 30% HF, and cellulose removal *via* acetolysis reactions. Samples were mounted with liquid glycerol and sealed permanently with paraffin wax. Pollen identification was conducted under a stereomicroscope at 400 fold magnification with the assistance of the Heusser (1971) pollen catalogue. A total of 100-250 terrestrial pollen grains were counted on each sample depending on their abundance. Pollen percentage for each taxon was calculated from the total sum of terrestrial pollen. The percentage of aquatic pollen and fern spores was calculated based on the total terrestrial sum plus their respective group. Pollen percentage diagrams were generated using the Tilia software (E. Grimm, Illinois State Museum, Springfield, IL. USA). The diagram was divided into "zones" based on the identification of the most important changes in pollen percentage and assisted by a cluster ordination (CONISS) performed by the same software.

We further summarize pollen-based precipitation trends by calculating a Pollen Moisture Index (PMI), which is defined as the normalized ratio between Euphorbiaceae (wet coastal scrubland) and Chenopodiaceae (arid scrubland). Thus, positive (negative) values of this index indicate the relative expansion (reduction) of coastal scrubland under relatively wetter (drier) conditions.

4. Results

4.1. Geochronology

$^{210}Pb_{xs}$ (unsupported activity) was obtained from the surface down to 8 cm depth in the two cores, with an age of ~ AD 1860 at 8 cm in both of them (Table S1). Greater surface activities were obtained for core BGGC5 (13.48 ± 0.41 dpm g^{-1}) compared to core

BTGC8 (5.80 ± 0.19 dpm g^{-1}), showing an exponential decay with depth (Fig. 4). A recent sedimentation rate of 0.11±0.01 cm yr^{-1} was estimated.

The age model provided a maximum age of cal BP 8210 for core BGGC5, and cal BP 7941 for core BTGC8 (Fig. 4). A mean sedimentation rate of 0.02 cm yr^{-1} was estimated for core BGGC5, with a period of relative low values (0.01 cm yr^{-1}) between cal BP ~4000 and 6000. For BTGC8, sedimentation rates were less variable and around 0.013 cm yr^{-1} in the entire core. An age reservoir estimation following the methodology of Sabatier et al. (2010) resulting in, 441 ± 35 and 442 ± 27 years for BGGC5 and BTGC8 cores, respectively (Table 3). These values were close to global marine reservoir and higher than other estimations along Chilean margin at shallower depths (146 ± 25 years at < 30 water depth; Carré et al., 2016; Merino-Campos et al., 2018). Our cores sites are deeper (~90 m water depth) receiving the influence of upwelled water from Lengua de Vaca Point, which could explain such differences. However, moderated differences were observed between models using these different reservoir values. Thus, our estimations were based on two pre-bomb values established with ^{210}Pb measured in sediments and ^{14}C in foraminifers, used for the age modeling.

4.2. Geophysical characterization

The sediments retrieved from the bays showed fine grains in the range of very fine sand and silt in the southern areas. There, the grain size distribution was mainly unimodal, very leptokurtic, better sorted and skewed to fine grain when compared to sediments from the northern areas. Sediment cores obtained from the northern areas were sandy (coarse sand and gravel), with abundant calcareous debris. Longer cores of soft sediment were retrieved at the southern areas (BGGC5 and BTGC8), where the silty component varied between 40 % and 60 % (Fig. 1 and 5a,b). The clay component was very low at both cores (<2%). The sediment's color ranged from very dark grayish brown to dark olive brown (2.5Y 3/3−3/2) at Guanaqueros Bay (BGGC5) and from dark olive gray to olive gray (5Y 3/2−4/2) at Tongoy Bay (BTGC8). Visible macro-remains (snails and fish vertebrae) were found and weak laminations were identified at both cores. The magnetic susceptibility showed higher values close to the surface, up to 127 SI $x10^{-8}$ at BGGC5 and relative lower values (85 SI $x10^{-8}$) at BTGC8. At greater depths, however, the values were very constant, around 5−8 $x10^{-8}$ SI at BGGC5 core and around 12−20 $x10^{-8}$ SI at BTGC8 core. In both cores, susceptibility increases substantially in the last century (Figs. 5a, 5b). Lower bulk densities were estimated at the core BGGC5 (0.7−0.9 g cm^{-3})

compared to the core BTGC8 (>1 g cm^{-3}) (Fig. 5a, 5b). In accordance with this, the mean grain size was 60−80 µm at Guanaqueros Bay (BTGC8), compared to 50−60 µm at Tongoy Bay (BGGC5). Both cores were negatively skewed, with values of -1 to -1.2 at BGGC5, and -1 to -2.5 at BTGC8. Minor increases towards coarser grain size were observed in the last 2000 years, especially at Tongoy Bay (BTGC8). In both cases, grain size distributions were strongly leptokurtic. Ca/Fe ratio also diminished in time, except at core BTGC8 where it was only observed during the last ~2000 years.

4.3. Biogenic components

4.3.1. Siliceous microfossils and biogenic opal

Total diatom abundance fluctuated between 5.52 x10^5 and 4.48 x10^7 valves g^{-1} in core BGGC5. Total diatom abundance showed a good correlation with biogenic opal content at BGGC5 (R^2 =0.52, P<0.5), with values increasing from 72 cm to the bottom of the core, corresponding to cal BP 5330, reaching highest values before cal BP 6500. In contrast, diatom abundance and biogenic opal were much lower in core BTGC8 (< 2 ×10^5 valves g^{-1} and <3%, respectively). Here, the siliceous assemblage was almost completely conformed by *Chaetoceros* resting spores (RS) (Fig. 6).

A total of 135 and 8 diatom taxa were identified in cores BGGC5 and BTGC8 respectively, where the core BTGC8 registered very low abundances of diatoms. In general, diatoms were the most important assemblage of siliceous microfossils (96%), followed by sponge spicules (3%). The contribution of phytoliths and chrysophyte cysts was less than 2% in core BGGC5. *Chaetoceros* (RS) dominated the diatom assemblage (~90%; Fig. 6), and included the species *C. radicans*, *C. cinctus*, *C. constrictus*, *C. vanheurckii*, *C. coronatus*, *C. diadema*, and *C. debilis*. Other species recorded of upwelling group (mainly in core BGGC5) were: *Skeletonema japonicum*, and *Thalassionema nitzschioides* var. *nitzschioides* (Table S2). Freshwater diatoms (*Diploneis papula*, *Cymbella tumida*, *Fragilaria capucina*, *Diatoma elongatum)* and non-planktonic diatoms (*Cocconeis scutellum*, *C. costata and Gramatophora angulosa*) accounted for ~0.1−5%; while the group of coastal planktonic diatoms accounted for ~0.3−6% of the total assemblage. The main planktonic diatoms were (*Rhizosolenia imbricata*, and *Thalassiosira eccentrica*). Oceanic-warm diatoms (*Roperia tesselata*, *Th. nitzschioides var inflatula)* and the tycoplanktonic diatom group were rare with less than 1%.

4.3.2. TOC and stable isotopes distribution

Consistent with opal and diatoms, core BGGC5 showed higher values of TOC (between 2 % and 5 %) compared with less than ~1.5 % in core BTGC8 (Fig. 5a,b). Furthermore, $\delta^{13}C$ was slightly higher at core BTGC8 (-20 ‰ to -21 ‰) compared with core BGGC5 (-21 ‰ to -22 ‰), the former also showing slightly increased values of $\delta^{15}N$ from the deeper sections to the surface of the core (<7 ‰ to >10 ‰). This increase was less evident at core BGGC5, with values of ~9 ‰ at depth to >10 ‰ on the surface (Fig. 5a,b). Diminishing TOC contents was related to slightly higher $\delta^{13}C$ values (~ -20 ‰) in both cores.

4.3.3. Pollen record

Initial surveys on core BTGC8 (Tongoy Bay) revealed extremely low pollen abundances which hampered further palynology work. A comprehensive pollen analysis was only conducted for core BGGC5 (Guanaqueros Bay). The pollen record of core BGGC5 consisted of 29 samples shown in Figure 7. The record was divided in five general zones following visual observation of changes in the main pollen types and also assisted by the cluster analysis CONISS.

Zone BG-1 (cal BP 8200 – 7600): This zone is dominated by the herbaceous taxa Chenopodiaceae, *Leucheria*-type, Asteraceae subfamily (subf.) Asteroideae, Apiaceae with overall high values of the wetland genus *Typha* spp.

Zone BG-2 (cal BP 7600 – 6500): This zone is also dominated by Chenopodiaceae, *Leucheria*-type and Asteraceae subf. Asteroideae. In addition, other non-arboreal elements such as *Ambrosia*-type, Poaceae, Brassicaceae and *Chorizanthe* spp. expand all considerably.

Zone BG-3 (cal BP 6500 –3400): This zone is marked by a steady decline in Chenopodiaceae and *Leucheria*-type, and by the expansion of several other herbaceous elements, such as Euphorbiaceae, *Baccharis*-type and Brassicaceae.

Zone BG-4 (cal BP 3400 – 120): This zone is mostly dominated by Ast. subf. Asteroideae, and marked by the decline of Chenopodiaceae and *Leucheria*-type. Other coastal taxa such as Euphorbiaceae, *Baccharis*-type, Asteraceae subf. Chichorioideae, *Quillaja saponaria*, Brassicaceae and *Salix* spp. also expand in this zone.

Zone BG-5 (cal BP 120 – -60): The upper portion of the record is dominated by Asteraceae subf. Asteroideae and Poaceae, and marked by increments of Geraniaceae, Asteraceae subf. Mutisieae, Myrtaceae and *Q. saponaria*. Additionally, this zone includes introduced pollen types such as *Rumex* spp. and *Pinus* spp. The latter is not shown in the diagram of Figure 8 because its abundance was minimal.

Overall, the most distinctive trend revealed in core BGGC-5 is a long-term decrease in Chenopodiaceae and increments in Euphorbiaceae and Asteraceae subf. Asteroideae. Along with these changes, a later expansion of several other pollen representatives of the coastal shrubland vegetation started at around cal BP 6500.

4.4. Trace element distributions

Trace element distributions are shown in figures 8a and 8b for Guanaqueros (BGGC5) and Tongoy Bays (BTGC8), respectively. Trace metals sensitive to the presence of oxygen (U, Re, Mo) showed increasing metal/Al ratios from the base of the core (cal BP ~8210) until cal BP 6500 in core BGGC5. After this maximum, ratios presented a slight increase towards cal BP 2000 close to the beginning of the recent era, followed by a sharp decrease until present. Similarly, the metal ratios in the core BTGC8 increase over time, yet the maximum was observed at cal BP ~1000. The exception of this trend was Mo which exhibited maximum values until cal BC 6000 and then a steady decrease towards the present. Additionally, metal/Al values were higher at core BGGC5. Iron displayed a clear increase around cal BP 3300 – 4000 at core BGGC5, not observed at core of Tongoy, instead it showed an increase around cal BP 6500 –7800 . Manganese did not show any clear trend.

A second element group (metal/Al ratios), including Cd, Ni and P (related to primary productivity and organic fluxes), showed a similar pattern than Mo/Al towards the bottom of core BGGC5, i.e. the highest values around cal BP 6500 and a constant reduction towards the present. A third group, consisting of Ba, P and Ca, exhibited a less clear pattern. The Cd/Al and Ni/Al ratios in core BTGC8 showed only slightly decreasing values, and the maximum values were very low compared to the BGGC5 core. The same pattern is observed for other elements. Metal/Al ratios for Ba, Ca and P were lower and presented a long-term decreasing pattern towards the present.

An exception to the previously described patterns was Cu/Al, which peaked at cal BP ~3600 – 3700 and showed a conspicuous increase in the past ~150 years. This was also observed at core BTGC8, but with lower concentrations than at core BGGC5.

5. Discussion

5.1. Sedimentary composition of the cores: terrestrial *versus* biogenic inputs

The sediments in the southern zones of the bays constitute a sink of fine particles transported from northern areas and the shelf (Fig. 5a, 5b), responding to the water circulation in the Guanaqueros and Coquimbo Bays described as bipolar, i.e. two counter-rotating gyres which are counterclockwise to the north and clockwise to the south (Valle-Levinson and Moraga, 2006). This is the result of the wind and a coastline shape delimited by two prominent points to the north and south. In the case of Tongoy Bay (the southernmost bay of the system), circulation shows a different pattern due to its northern direction compared to Guanaqueros Bay, which opens to the west. The cyclonic recirculation in Tongoy Bay seems to be part of a gyre larger than the Bay's circulation (Moraga et al., 2011). This could explain differences in sediment particle distribution and composition between the bays. At Tongoy Bay, there are less organic carbon accumulation (< 3 g m^{-2} yr^{-1}), siliceous microfossils and pollen (Figs. 5b, 6 and 7). Similarly, in Guanaqueros Bay TOC contents are only slightly higher (> 2 %), especially between cal BP 3700 and 4000 and before cal BP 6500 (~ 4 %) but higher accumulation rates around 7 and 16 g $m^{-2}yr^{-1}$, respectively (Fig. 5a). However, sediments there contain enough microfossils to establish differences in primary productivity periods and also provide a pollen record evidencing the prevailing environmental conditions.

The stable isotopes measured in the study area were in the range of marine sedimentary particles for southern oceans at low and mid latitudes ($\delta^{13}C$; -20 ‰ – -24 ‰; Williams 1970; Rau et al., 1989; Ogrinc et. al. 2005), and slightly lower than the TOC composition at the water column (-18 ‰, Fig. 3). This suggests that the organic particles that settle on the bottom are a more refractory material (C/N: 9−11), remineralized during particle transportation and sedimentation. This results in lighter isotopic compositions, especially at core BTGC8. Furthermore, the $\delta^{15}N$ and $\delta^{13}C$ of settled particles are more negative at surface sediments due to a preferential degradation of molecules rich in ^{13}C and ^{15}N, resulting in more negative values and higher C/N ratios at sediments than in suspended particles (Fig. 3, 5a, 5b). However, this is also due to the stronger diagenetic reactions observed near the bottom layer (Nakanishi and Minagawa, 2003). Thus, these sediments are composed by winnowed particles transported by water circulating over the shelf, and the isotopic variations should not establish clearly the contribution of terrestrial inputs.

Otherwise, the isotopic composition of upwelled NO_3 (De Pol-Holz et al., 2007) could influence the variability of $\delta^{15}N$. Values for $\delta^{15}N$ at northern and central Chile are in the range of those measured at BGGC5 core (~11‰; Hebbeln et al., 2000, De Pol-Holz et al., 2007), resulting by the isotopic fractionation of NO_3 during nitrate reduction within OMZ leaving a remnant NO_3 enriched in ^{15}N (Sigman et al., 2009; Ganeshram et al., 2000 and references therein). In this case, the BGGC5 core sediments represent the effect of the nutrient supply by the upwelling and the influence of the OMZ over the shelf resulting in $\delta^{15}N$ of 9 − 10‰. At BTGC8 sediment core, lower values (<8‰) at greater depths within the core should represent the mixing with light terrestrial organic material (Sweeney and Kaplan, 1980), due to the nearest position of a permanent small wetland at southern site of Tongoy Bay. Pachingo wetland material showed $\delta^{15}N$ of 1 − 8‰ (Muñoz et al., data will be published elsewhere) in the range of sedimentary environments influenced by terrestrial runoff (Sigman et al., 2009). In the same sense, at most of the cases, lower TOC is correspondingly with lighter $\delta^{15}N$ values, and also with the highest C/N ratios suggesting the mixing with continental material (Fig. 5b).

Magnetic susceptibility (MS) measurements revealed lower values throughout both cores (BGGC5: 5 – 8 $x10^{-8}$ SI; BTGC8: 12 – 20 $x10^{-8}$ SI), except at dates of the last ~100 years (CE 1800), when it increases substantially to values similar to those observed in the Pachingo wetland (40 – ~200 $x10^{-8}$ SI; unpublished data) on the southern side of Tongoy Bay. Magnetite has strong response to magnetic fields and its concentration is considered proportional to magnetic susceptibility (Dearing, 1999). Additionally, mineral post-depositional transformations (alteration of magnetite minerals) and dilution by biogenic components (carbonates, silicates) should also be relevant in the MS intensity in zones with high organic accumulation rates (Hatfield and Stoner, 2013). However, this is not expected to be the case for our cores and the MS should be mainly accounting for the source of the particles. The highest MS measurements on surface sediments would indicate a greater contribution of terrestrial material. The area is surrounded by several creeks that are only active during major flooding events, with greater impacts on Tongoy Bay compared to Guanaqueros Bay. An important increment in the contribution of terrestrial material has occurred in Tongoy Bay in recent times (Ortega et al., in review), which is diluting organic proxy records and increasing the grain size. Our records indicate a slight increase in mean grain size at both bays, supported also by a slight decrease in Ca/Fe ratio indicating more Fe input from continental erosion (Fig. 5a, 5b).

Recent information indicates that during the intensification of southern winds the upwelling develops a nutrient-rich and low-oxygen flow within the bay's southern areas (Gallardo et al., 2017), which promotes phytoplankton blooms and low oxygen events. Decreasing concentrations of Ca from the deepest part of both cores to the surface was interpreted as decreasing primary productivity (Keshav and Achyuthan, 2015; Sun et al., 2016), but higher concentrations were measured in core BGGC5 compared with core BTGC8, where more terrestrial influence is being suggested. The slight increase of K/Ca ratio in time, from bottom to the surface, should also be interpreted as a slight increase in continental input, since K is related to siliciclastic material from coastal erosion, fluvial and groundwater inputs. However, the variation of Ca was larger (Fig.6a, 6b), resulting in higher K/Ca ratios at the surface. This indicating that the continental input has not changed much in time but rather the primary productivity has decreased (Fig. 5a, 5b).

5.2. Temporal variability of proxies for primary productivity

Several elements participating in phytoplankton growth are useful to interpret variations in primary productivity in time, as they are preserved in the sediments under suboxic-anoxic conditions. This produces enrichment over crustal abundance, which distinguishes them from continental inputs. The presence of free dissolved sulfides produced by sulfate reduction reactions in the diagenesis of organic matter allows for the precipitation of metals on the pore water (Calvert and Pedersen, 1993; Morse and Luther, 1999). At the same time, organic matter remineralization releases ions to the pore water where they could form organic complexes and insoluble metal sulfides. Conversely, they could be incorporated into pyrite as Cd, Ni and Cu, showing different degrees of trace metal pyritization (Huerta-Diaz and Morse, 1992). Ca, Sr, Cd and Ni profiles suggest a lower proportion of organic deposition in time (Fig. 8a, 8b), consistent with the slight reduction of TOC content observed in the sediments (Figs. 5a, 5b), and concomitantly with other elements related to organic fluxes to the bottom and primary productivity. In the case of Ba, it is actively incorporated into phytoplankton biomass or adsorbed onto Fe oxyhydroxides, increasing the Ba flux towards the sediments, where it is also released during organic matter diagenesis. Ba is precipitating in microenvironments where Ba-sulfate reaches supersaturation (Tribovillard et al., 2006 and references therein), but it is dissolved in suboxic-anoxic environments or where sulfate is significantly depleted (Torres et al., 1996; Dymond et al., 1992). Therefore, it is better preserved in less anoxic environments with moderate productivity, expected to be the case of our study site (Gross Primary Productivity =0.35 to 2.9 g C $m^{-1}d^{-1}$; Daneri et al., 2000). Hence, the slight increase of Ba from cal BP 4000 to the present (Fig. 8a) should rather be the response to a less anoxic environment than to an increase in primary productivity and results in a low negative correlation with TOC (-0.59; Table 4) due to the Ba remobilization in anoxic conditions before cal BP 6500. After this age, the reduction in TOC and other nutrient-type elements (Ni, Sr, Ca, Cd) to the present is consistent with the increase in oxygen at the bottoms. On the other hand, P distribution showed a trend similar to that of TOC and other elements related to organic fluxes to the bottom (Ni, Cd), although with a lower correlation (~0.6). The accumulation of P depends on the deposition rate of organic P (dead plankton, bones and fish scales) to the bottom, and is actively remineralized during aerobic or anaerobic bacterial activity. Dissolved P diffuses towards the water column where part of it could be adsorbed onto Fe oxides that maintain this element within the sediments. P is buried during a continued sedimentation process and could be released to the pore water under anoxic conditions, when oxides are reduced, creating the environmental conditions for phosphorite and carbonate-fluorapatite precipitation. Normally, this takes place in sites with high sedimentation rates and high organic matter fluxes to the bottom (Filippelli, 1997; Cha et al., 2005), which was not the case for our study area (<0.02 cm yr^{-1}). In spite of this difference, P and TOC showed a decreasing trend towards the present, suggesting reducing flux of organic matter over time, which was also observed for Ni and Cd distributions. Alternatively, it could be explained by the increased remineralization of the organic material settled on the bottom (Figs. 8a, 8b).

Productivity reconstructions were based on diatom relative abundances and biogenic opal content only in core BGGC5, since core BTGC8 registered valve counts that were too low (<1% in relative diatom abundance). However, at both cores diatom assemblages were represented mainly by *Chaetoceros resting spores*, which are used as upwelling indicators, showing increased concentrations during periods of high productivity and upwelling (Abrantes 1988, Vargas et al., 2004). In addition, *Chaetoceros* resting spores are highly silicified and well preserved in coastal sediments (Blasco et al., 1981). The downcore siliceous productivity based on opal distribution (Fig. 6) distinguished three main periods of increased productivity: (1) > cal BP 6500,

(2) cal BP 2100 – cal BP 4600 and (3) recent time (CE 2015) – cal BP ~260. The mean opal accumulation rate in the second period was 12 ± 5 g m^2 yr^{-1}, when spicules and minerals (quarz, framboid pyrite) where abundant in smear slides. During the first period, accumulation increased noticeably to ~30 ± 15 g m^2 yr^{-1}, when the *Chaetoceros* spores were predominant, indicating upwelling intensification and low spicules and minerals were observed in the slides. This is partially consistent with the nutrient–type element distributions. Although the third period was too short, high opal accumulation and high Cd/U ratios could also be observed, which increased toward the present (mean opal value of 32 ± 22 g m^2 yr^{-1}). Similarly, Cu and Fe also increased in recent times (Fig. 8a), contributing to fertilize the environment and promoting primary productivity. The second period was not clearly identified in terms of metals, except for Fe which shows a conspicuous increment in this period (Fig. 8a). During the first period, all metal proxies showed primary productivity increases before cal BP 6500, as indicated by opal accumulation within the sediments. In anoxic-suboxic environments Cd/U ratios could vary between 0.2 and 2 (Nameroff et al., 2002), the high concentrations of both elements reflect anoxic conditions but their different behavior could result in variable Cd/U ratios in suboxic environments. Here, the Cd and U accumulation on sediments resulted in high Cd/U ratios (>2; Fig. 6) during periods with high opal accumulation in the cores, especially in the first period, and even in core BTGC8; and lower ratios (< 1; Fig. 6) when opal was low, indicating higher variations in the primary productivity in time with moderated changes in oxygen conditions at the bottoms. Opal showed good correlations with Ni and Cd (˜0.70; Table 4; Fig. 8a), all suggesting the relevance of bottom organic fluxes for element accumulation within the sediments, and establishing a clear period of higher primary productivity around cal BP 6500, when lowest oxygen conditions prevailed (Fig. 6).

5.3. Temporal variability of proxies for bottom water oxygenation

U, Re and Mo distributions in core BGGC5 indicate that anoxic or suboxic conditions were developed from cal BP 8200 to ~ cal BP 2000. After this period and towards the present, however, a remarkable reduction in their concentration suggests a more oxygenated bottom environment, concurrent with lower organic fluxes to the sediments. The Re profile shows the influence of suboxic waters not necessarily associated with increased organic matter fluxes to the bottom. Since this element is not scavenged by organic particles, its variability is directly related to oxygen changes (Calvert and Pedersen, 2007, and references therein). Additionally, it is strongly enriched above crustal abundance in suboxic conditions (Colodner et al., 1993; Crusius et al 1996), being >10 times in core BGGC5 (Table 5) before cal BP 2000. In the same way, U exhibits a similar pattern, and although organic deposition has an impact on its distribution (Zheng et al., 2002), it also relates to changes in bottom oxygen conditions. This is because its shift from a soluble conservative behavior to non-conservative and insoluble behavior solely depends on the redox potential change that occurs near the Fe(III) reduction zone (Klinkhammer and Palmer, 1991). Molybdenum, which showed high increases at cal BP 6500, also indicates the presence of sulfidic conditions, as shown by the Re distribution highly enriched in anoxic environments (Colodner et al., 1993), and by the reduction of Re(VII) to Re(IV) forming ReO_2 or ReS (Calvert and Pedersen, 2007). Rhenium, U and Mo enrichment are used to decipher the redox condition within the sediments, even in places with high lithogenic input that could obscure the authigenic enrichment of other elements under similar conditions (Crusius et al., 1996). In both places, the concentrations of these elements showed values above the crustal abundance, especially in core BGGC5 (Table 3), with Re and Mo becoming more enriched (>13) than U (~ 5), except at recent time that diminish drastically. This suggests that the presence of anoxic conditions were stronger around cal BP 6500 – 7200 whit a peak at cal BP 6500 and a second peak at cal BP 2100. The most important enrichment was observed for Cd (> 30) but higher before cal BP 6500 (~147) in agrement with higher opal accumulation and diatoms (Table 5). The most important enrichment could similarly indicate the sulfidic condition within the sediments that allows Cd precipitation. It is also supported by Mo enrichment, since its accumulation within the sediments is highly controlled by sulfide concentrations (Chaillou et al., 2002; Nameroff et al., 2002; Sundby et al., 2004).

Something similar occurs in Tongoy Bay (core BTGC8), but trace metal concentrations are lower for all elements and also for TOC, suggesting that it has limited influence on metal accumulation within the sediments.

Thus, these elements suggest anoxic conditions within the sediments in both places around cal BP 6500 − 7200 (Fig. 8a, 8b). After this period, a second maximum but less intense anoxia is observed at the beginning of the recent era (cal BP 2000), continuing with a conspicuous oxygenation until present times. This interpretation based on the distribution of U, Re and Mo complements the observations of nutrient-type elements pointing both to oxygenation changes and to changes in organic fluxes thorough the sediments. A less prominent accumulation of nutrient-type elements (Ni, Cd, Ba, Ca and P) would indicate lower organic material deposition to the sediments but promoting anoxic conditions within the sediments and lower sulfide content with time, which are nevertheless high enough to sustain Mo accumulation until cal BP 2000. After that, a notorious decrease in Re, U and Mo accumulation and lower EFs were observed, suggesting that the oxygenation of the bottom becomes relevant (Table 5). This could also explain the conspicuous increase of Cu/Al and Fe/Al in recent times due to the presence of oxides (Fig. 8a, 8b). Apparently, a low level of dissolved Cu is maintained by the complexation with organic compounds produced by phytoplankton and Cu adsorption on Fe oxides (Peacock and Sherman, 2004; Vance et al., 2008; Little et al., 2014), with both processes increasing Cu in the particulate phase over surface sediments. At our study sites, Fe and Cu concentrations were higher in surface sediments, probably related to an increase in Fe and Cu availability in the environment (Fig. 8a, 8b). This could be in turn associated with mining activities carried out in the area since the beginning of cal BP 13 (AD 1937).

At present, the suboxic conditions within the bays result from the influence of adjacent water masses with low oxygen contents, related to the oxygen minimum zone (OMZ) (Fig. 2) centered at ~250 m. Upwelling promotes the intrusion of these waters towards the bays, with strong seasonality. Transition times develop in short periods by changes in wind directions and intensities along the coast. Additionally, oceanic variability along the western coast of South America is influenced by equatorial Kelvin waves on a variety of timescales, from intraseasonal (Shaffer et al.,1997) and seasonal (Pizarro et al., 2002; Ramos et al., 2006) to interannual (Pizarro et al., 2002; Ramos et al., 2008). Coastal-trapped Kelvin waves originating from the equator can propagate along the coast, modify the stability of the regional current system and the pycnocline, and trigger extratropical Rossby waves (Pizarro et al., 2002; Ramos et al., 2006; 2008). This oceanographic feature will generate changes in oxygen content within the bays with major impacts on redox sensitive elements in surface sediments; thus, the increased frequency and intensity of this variability would result in a mean effect which is observed as a gradual change in metal contents in time.

5.4. Climatic interpretations

The present-day climate of the semi-arid region of Chile is largely influenced by the position of the Southeast Pacific Subtropical Anticyclone (SPSA) and latitudinal displacements of the Southern Westerly Winds (SWW). The dynamic of these large-scale atmospheric systems, from seasonal to decadal timescales, control the amount of precipitation that reaches this region. Because the semi-arid region of Chile represent the northernmost area under the influence of the SWW, precipitation is relatively scarce and restricted to the austral winter months when the SPSA and SWW shift northwards, bringing precipitation fronts to the semiarid coast and the interior land (Montecinos and Aceituno, 2003; Quintana and Aceituno, 2012).

In accordance with the modern climatology, paleoenvironmental records from the semiarid region have mostly been interpreted to reflect past variability in the intensity and latitudinal position of the SWW. In this regard, the Holocene period features a series of wet and dry phases resulting from millennial-scale SWW changes (Hebbeln et al., 2002; Lamy et al., 1999; Maldonado and Villagrán, 2002). In particular, pollen records from the southern coastal areas of Coquimbo (32°S) indicate that wet conditions predominated before cal BP 8700, which brought the expansion of swamp forests areas along the coast (Maldonado and Rozas, 2008; Maldonado and Villagrán, 2006). This scenario occurred concomitantly with diminished rainfalls, regional aridity and strong southerly winds consistently with La Niña-like conditions prevailing during the Early Holocene along the arid and semiarid coasts of Chile (Vargas et al., 2006; Ortega et al., 2012), that would have driven increased coastal humidity associated to coastal fogs favored also by a relatively low sea level position with respecto to the present (Ortega et al., 2012). This wet period was followed by a long-lasting arid phase between cal BP 8700 and 5700. Regional aridity matches the relative dry conditions detected in the first portion of our pollen reconstruction from core BGGC5 in the Guanaqueros Bay, which is represented by relative low values of the Pollen Moisture Index in Fig. 9. Similarly, a general increase in regional precipitation after cal BP ~6000, observed in pollen records from the northern margin of SWW (Jenny et al., 2003; Maldonado and Villagrán, 2006) is broadly correlated with the observed long-term trend towards increased precipitation observed in the Pollen Moisture after cal BP ~6500 − 6700. This is also in agreement with Al and Pb, usually considered to be indicators of continental particles that enter to marine waters by fluvial or aerial transport (Calvert and Pedersen, 2007; Govin et al., 2012; Ohnemus and Lam, 2015; Saito et al., 1992; Xu et al., 2015). In our cores, these elements showed trend similar to the pollen record, i.e., a gradual rise in time, suggesting increased humid conditions during recent periods (Fig.9).

In addition, our records indicate long-term increases in grain size and K/Ca ratios and Fe over the last ~8000 years. These increases point to a higher continental inputs most probably caused by increasing rainfall events, which are an important source of sands and K in the northern Chilean margin at the present. At a regional scale, a trend towards increasing precipitations is also consistent with the occurrence of alluvial episodes since 8600 cal. BP, after a period of an almost quiescence of this phenomenon in the coastal region located just to the south of Tongoy bay (Ortega et al., 2012). Increments of Fe have been documented to provide a boost in primary productivity analyzed in sedimentary records (Dezileau et al., 2004). In our cores, a short-term increase in Fe concentrations is observed between cal BP ~4000 – 3300 at the Guanaqueros core, whereas persistent high values are recorded in the Tongoy core between cal BP 6500 – 7800. These two increases coincide with periods with relatively high primary productivity based on the diatoms and opal distribution (Figs. 6, 8b). This correlation supports the role of Fe as promoter of coastal productivity in the past. However, we note that maximum productivity observed at cal BP ~6500 seems at odd with the overall dry environmental conditions evidence by the pollen data. An explanation for this discrepancy is that dry conditions were more likely associated with increases in SPSH activity in the region and consequently with higher upwelling (Frugone-Álvarez et al., 2017). The subsequent weakening in paleoproductivity after cal BP 6500 can be explained by a reduction in upwelling due to reduced SPSH activity and by the intrusion of less nutrient-enriched upwelled waters over the shelf, influenced by remote equatorial waves, as it is observed today. It is important also to considerate a possible influence of a sea level located in a lower position with respect to its present day position before 7000-6000 cal BP (Lambeck et al., 2014), that would have influenced productivity variations and also its recording at the sea bottom in these bays. The oldest transgressive deposits at Coquimbo Bay dated from BP 6380 and a gradual progradation of the coast from BP 2500 until present (Ota and Paskoff, 1993), changes the dynamic of the depositional environments due to a greater continental influence, observable in our cores.

The synchronism between highest productivity and dry conditions prior to ~cal BP 6500 highlights the role of the SPSA as an important driver of paleoproductivity changes in the coast of semi-arid Chile during the early portion of the Holocene Period. On the other hand, the pollen and trace element record show both a coherent pattern of increasing humidity and continental discharge over the last 7000 years. The driver of this long-term paleoclimate trend seems to be associated with past shifts in the position of the SWW. In particular, an equatorial displacement of the SWW during mid and later part of the Holocene period has been suggested by reconstructions from terrestrial and marine proxies (Veit, 1996; Lamy et al., 1999; Lamy et al. 2010).

Studies of coastal upwelling from the Central Peruvian and south Central Chilean coasts (12 − 36 °S) show that present-day wet/dry variability associated with El Niño Southern Oscillation exert an important influence on the bottom ocean oxygenation (Escribano et al., 2004; Gutiérrez et al., 2008; Sellanes et al., 2007). In this regard, OMZs is expected to be less intense during warm El Niño phases and vice versa. This link has been observed by recent studies, as warm events in the Tropical Pacific tend to be associated with low productivity and weak OMZ in the Peruvian coast (Salvatteci et al., 2014). An increase in the frequency of ENSO-like warm events could partly explain the reduction in productivity recorded after cal BP 6700 in our records, concomitantly with the coastal progradation (Ota and Paskoff, 1993). In this case, warm events in the eastern Pacific could have reduced the ocean productivity and organic fluxes from primary productivity and overall dropping oxygen consumption during organic matter diagenesis. In the light of these mechanisms, our results suggest more El Niño-like conditions during the latter part of the Holocene, an inference that is consistent with the available evidence for an increase in the frequency of El Niño events over the last 4000–5000 years (Conroy et al., 2008; Moy et al., 2002). We further note that present-day El Niño years are generally connected with increased westerly flow over central Chile including the semi-arid region (Montecinos and Aceituno, 2003), and therefore more frequent El Niño states during the latter part of the Holocene are also consistent with a long-term increase in precipitation revealed by the pollen and trace element data.

6. Conclusions

Our result indicates that the ocean circulation at our study sites seems to affect both places differently, leaving more variable grain compositions and higher TOC contents in the Guanaqueros Bay (core BGGC5) than in the Tongoy Bay (core BTGC8). This difference should be interpreted as an increase in the time of particle transportation resulting in grain size selection (more leptokurtic at core BTGC8), especially after cal BP 2000. Furthermore, in both bays, constantly decreasing TOC contents were observed after cal BP ~4000 to the present, probably due to higher oxygenation of the bay bottom in time.

Differences in redox conditions in our records could be reconstructed in detail, showing a clear decreasing trend in oxygen bottoms before the beginning of recent time (cal BP ~2000), followed by a rapid change to a more oxygenated environment. The environmental conditions at bottom waters was essential in the metal enrichment factor above crustal abundance within the sediments (highest EFs), since low organic carbon accumulation and low sedimentation rates have been estimated, indicating that the accumulation of these elements (U, Mo and Re) depends mainly on oxygen content instead of on organic carbon burial rates. Our result suggest that a maximum suboxia-anoxia occurred at cal BP ~6500, when peak U and Re where recorded, probably due to the presence of a sulfidic environment.

The nutrient-type elements follow a similar trend, reduced at present and showing higher accumulation rates around cal BP 6500 (Ca, Ni, P and Cd). Their distribution is consistent with the diatom and opal distributions, showing their dependence on primary productivity and organic carbon burial rates. If the kinetics reaction is working at low rates for these elements, they should be highly influenced during oxygenation periods, something that seems to have been operating at higher frequencies.

The record of continental proxies suggests a long-term increase in precipitation, consistent with previous reconstructions in central Chile. The most distinctive changes were observed after cal BP 6500 – 6700 when an overall expansion of the coastal vegetation occurred as a result of a progressive increase in precipitation and river runoffs concomitantly with a gradual coastal progradation, expanding the grain size of the sediments and the higher concentrations of elements with an important continental source (Al, Fe, K and Pb).

Increased regional precipitations amounts have been commonly interpreted by a northward shift of the Southern Westerly Winds belts, yet the increased frequency of El Niño events did more likely introduce a high variability of humidity after cal BP 5000. Thus, the apparent increase of oxygen conditions at bottoms could have been the result of this oceanographic feature, which introduced a more oxygenated water mass to the shelf and bays, temporarily changing the redox conditions in surface sediments and affecting the sensitive elements to redox potential change in the environment. Additionally, this also affected the accumulation of organic matter due to an intensification of its remineralization, showing a decreasing trend in nutrient type element accumulation and organic carbon burial rates towards the present. Finally, our results suggest that the geochemistry and sedimentary properties of coastal shelf environments in North-central Chile have changed considerably during the Holocene period. In particular, decreasing trends in primary productivity highlight the sensitivity of these environments to regional climate changes at different timescales. Future changes are therefore likely to be expected in the ongoing scenario of environmental changes at unprecedented rates.

7. References

Abrantes, F.: Diatom assemblages as upwelling indicators in surface sediments off Portugal, Mar. Geol., 85(1), 15–39, doi:10.1016/0025-3227(88)90082-5, 1988.

Ancapichún, S., Garcés-Vargas, J.: Variability of the Southeast Pacific Subtropical Anticyclone and its impact on sea surface temperature off north-central Chile Variabilidad del Anticiclón Subtropical del Pacífico Sudeste y su impacto sobre la temperatura superficial del mar frente a la costa centro-norte de Chile, Cienc. Mar., 41(1), 1–20, http://dx.doi.org/10.7773/cm.v41i1.2338, 2015.

Appleby, P. G. and Oldfield, F.: The calculation of lead-210 dates assuming a constant rate of supply of unsupported210Pb to the sediment, Catena, 5(1), 1–8, doi:10.1016/S0341-8162(78)80002-2, 1978.

Behrenfeld, M. J., O'Malley, R. T., Siegel, D. A., McClain, C. R., Sarmiento, J. L., Feldman, G. C., Milligan, A. J., Falkowski, P. G., Letelier, R. M. and Boss, E. S.: Climate-driven trends in contemporary ocean productivity, Nature, 444(7120), 752–755, doi:10.1038/nature05317, 2006.

Bevington, P. and Robinson, K. (Eds.): Error analysis. In: Data Reduction and Error Analysis for the Physical Sciences, WCB/McGraw-Hill, USA, 38–52, 1992

Blasco, D., Estrada, M. and Jones, B. H.: Short time variability of phytoplankton populations in upwelling regions-the example of Northwest Africa. In: Coastal upwelling. F. A. Richards (Ed.), AGU Washington DC, 339 – 347, 1981

Blott, S. J. and Pye, K.: Gradistat: A Grain Size Distribution and Statistics Package for the Analysis of Unconcolidated Sediments, Earth Surf. Process. Landforms, 26, 1237–1248, doi:10.1002/esp.261, 2001.

Calvert, S. E. and Pedersen, T. F.: Geochemistry of Recent oxic and anoxic marine sediments: Implications for the geological record, Mar. Geol., 113(1–2), 67–88, doi:10.1016/0025-3227(93)90150-T, 1993.

Calvert, S. E. and Pedersen, T. F.: Chapter Fourteen Elemental Proxies for Palaeoclimatic and Palaeoceanographic Variability in Marine Sediments: Interpretation and Application, Dev. Mar. Geol., 1(7), 567–644, doi:10.1016/S1572-5480(07)01019-6, 2007.

Carré, M., Jackson, D., Maldonado, A., Chase, B.M., Sachs, J.P.: Variability of 14C reservoir age and air–sea flux of CO2 in the Peru–Chile upwelling region during the past 12,000 years, Quat. Res., 85, 87–93, 2016.

Merino-Campos, V., De Pol-Holz, R. Southon, J., Latorre, C., Collado-Fabbri, S.: Marine radiocarbon reservoir age along the Chilean continental margin, Radiocarbon, 81, 1–16, doi:10.1017/RDC.2018.81, 2018.

Cha, H. J., Lee, C. B., Kim, B. S., Choi, M. S. and Ruttenberg, K. C.: Early diagenetic redistribution and burial of phosphorus in the sediments of the southwestern East Sea (Japan Sea), Mar. Geol., 216(3), 127–143, doi:10.1016/j.margeo.2005.02.001, 2005.

Chaillou, G., Anschutz, P., Lavaux, G., Schäfer, J. and Blanc, G.: The distribution of Mo, U, and Cd in relation to major redox species in muddy sediments of the Bay of Biscay, Mar. Chem., 80(1), 41–59, doi:10.1016/S0304-4203(02)00097-X, 2002.

Chester, R.: Redox environments and diagenesis in marine sediments, In: Marine Geochemistry, Chapman & Hall, 486‒524, 1990.

Colodner, D., Sachs, J., Ravizza, G., Turekian, K. K. and Boyle, E.: The geochemical cycle of Re: a reconnaissance, Earth Planet. Sci. Lett., 117, 205–221, doi:10.1016/0012-821X(93)90127-U, 1993.

Conroy, J.L., Overpeck, J.T., Cole, J.E., Shanahan, T.M., Steinitz-Kannan, M.: Holocene changes in eastern tropical Pacific climate inferred from a Galápagos lake sediment record. Quat. Sci. Rev., 27, 1166-1180, 2008.

Crusius, J., Calvert, S., Pedersen, T. and Sage, D.: Rhenium and molybdenum enrichments in sediments as indicators of oxic, suboxic and sulfidic conditions of deposition, Earth Planet. Sci. Lett., 145(1–4), 65–78, doi:10.1016/S0012-821X(96)00204-X, 1996.

Daneri, G., Dellarossa, V., Quiñones, R., Jacob, B., Montero, P. and Ulloa, O.: Primary production and community respiration in the Humboldt Current System off Chile and associated oceanic areas, Mar. Ecol. Prog. Ser., 197, 41–49, doi:10.3354/meps197041, 2000.

Dearing, J., Magnetic susceptibility. In: Environmental Magnetism: A Practical Guide. Walden, J., Oldfield, F., and Smith, J. (Eds.), Quaternary Research Association Technical Guide No. 6, London, 35–62, 1999.

De Pol-Holz, R., Ulloa, O., Lamy, F., Dezileau, L., Sabatier, P., and Hebbeln, D.: Late Quaternary variability of sedimentary nitrogen isotopes in the eastern South Pacific Ocean, Paleoceanography, 22, PA2207, doi: 10.1029/2006 PA001308, 2007.

Dezileau, L., Ulloa, O., Hebbeln, D., Lamy, F., Reyss, J. L. and Fontugne, M.: Iron control of past productivity in the coastal upwelling system off the Atacama Desert, Chile, Paleoceanography, 19(3), doi:10.1029/2004PA001006, 2004.

Dymond, J., Suess, E. and Lyle, M.: Barium in deep-sea sediment: A geochemical proxy for paleoproductivity, Paleoceanography, 7(2), 163‒181, 1992.

Escribano, R., Daneri, G., Farías, L., Gallardo, V. A., González, H. E., Gutiérrez, D., Lange, C. B., Morales, C. E., Pizarro, O., Ulloa, O. and Braun, M.: Biological and chemical consequences of the 1997-1998 El Niño in the Chilean coastal upwelling system: A synthesis, Deep. Res. Part II Top. Stud. Oceanogr., 51(20–21), 2389–2411, doi:10.1016/j.dsr2.2004.08.011, 2004.

Faegri, K. and Iversen, J.: Textbook of pollen analysis, IV. The Blackburn Press, New Yersey, 328 pp., 1989.

Filippelli, G. M.: Controls on phosphorus concentration and accumulation in oceanic sediments, Mar. Geol., 139, 231-240, 1997.

Flynn, W. W.: The determination of low levels of polonium-210 in environmental materials, Anal. Chim. Acta, 43, 221–227, 1968.

Frugone-Álvarez, M., Latorre, C., Giralt, S., Polanco-Martínez, J., Bernárdez, P., Oliva-Urcia, B., Maldonado, A., Carrevedo, M. L., Moreno, A., Delgado Huertas, A., Prego, R., Barreiro-Lostres, F. and Valero-Garcés, B.: A 7000-year high-resolution lake sediment record from coastal central Chile (Lago Vichuquén, 34°S): implications for past sea level and environmental variability, J. Quat. Sci., 32(6), 830–844, doi:10.1002/jqs.2936, 2017.

Gallardo, M.A., González, A., Ramos, M., Mujica, A., Muñoz, P., Sellanes, J., Yannicelli, B.: Reproductive patterns in demersal crustaceans from the upper boundary of the OMZ off north-central Chile, Cont. Shelf. Res. 141, 26–37, 2017. http://dx.doi.org/10.1016/j.csr.2017.04.011

Ganeshram, R.S., Pedersen, T. F., Calvert, S.G.,McNeill, G., Fontugne, M.: Glacial-interglacial variability in denitrification in the world's oceans: Causes and consequences. Paleoceanography, 15(4), 361– 376, 2000.

Garreaud, R. and Rutllant, J.: Análisis meteorológico de los aluviones de Antofagasta y Santiago de Chile en el período 1991–1993, Atmósfera, 9, 251–271, 1996.

Garreaud, R., Vuille. M., Compagnuccic, R. and Marengo, J.: Present-day South American climate, Palaeogeogr. Palaeocl., 281, 180-195, 2009 doi:10.1016/j.palaeo.2007.10.032

González, H. E., Daneri, G., Figueroa, D., Iriarte, J., Lefèvre, N., Pizarro, G., Quiñones, R., Sobarzo, M. and Troncoso, A.: Producción primaria y su destino en la trama trófica pelágica y océano profundo e intercambio océano-atmósfera de CO2 en la zona norte de la Corriente de Humboldt (23º S): posibles efectos del evento El Niño 1997. Rev. Chil. Hist. Nat., 71, 429-458, 1998.

Govin, A., Holzwarth, U., Heslop, D., Ford Keeling, L., Zabel, M., Mulitza, S., Collins, J. A. and Chiessi, C. M.: Distribution of major elements in Atlantic surface sediments (36°N-49°S): Imprint of terrigenous input and continental weathering, Geochemistry, Geophys. Geosystems, 13(1), 1–23, doi:10.1029/2011GC003785, 2012.

Guieu, C., Martin, J. M., Tankéré, S. P. C., Mousty, F., Trincherini, P., Bazot, M., Dai, M. H.: On trace metal geochemistry in the western Black Sea: Danube and shelf area. Estuarine, Coastal and Shelf Science, 47, 471–485, 1998.

Gitiérrez, D., Sifedine, A., Reyss, J.L., Vargas, G., Velazco, F., Salvattci, R., Ferreira, V., Ortlieb, L., Field, D., Baumgartner, T., Boussafir, M., Boucher, H., Valdés, J., Marinovic, L., Soler, P., Tapia, P: Anoxic sediments off Central Peru record interannual to multidecadal changes of climate and upwelling ecosystem during the last two centuries, Adv. Geosci. 6, 119–125, 2006.

Gutiérrez, D., Enríquez, E., Purca, S., Quipuzcoa, L., Marquina, R., Flores, G. and Graco, M.: Oxygenation episodes on the continental shelf of central Peru: Remote forcing and benthic ecosystem response. Prog. Oceanogr., 79, 177–189, 2008.

Gutiérrez, D., Sifeddine, A., Field, D. B.,, Ortlieb, L-., Vargas, G., Chávez, F.P., Velazco, F., Ferreira, V., Tapia, P., Salvatteci, R., Boucher, H., Morales, M.C., Valdés, J., Reyss, J.-L., Campusano, A., Boussafir, M., Mandeng-Yogo, M., García, M., Baumgartner, T.:Rapid reorganization in ocean biogeochemistry off Peru towards the end of the Little Ice Age, Biogeosciences, 6, 835–848, 2009.

Hansen, H. P., Koroleff, F.: Determination of nutrients. In Methods of Seawater Analysis. Grasshoff, K., Kremling, K. and Ehrhardt, M. (Eds.), Wiley-VCH Verlag GmbH, Weinheim, Germany, 159–228, 1999.

Hatfield, R. G., Stoner, J. S.: Magnetic Proxies and Susceptibility. In: The Encyclopedia of Quaternary Science. Elias, S.A. (ed.) 2, 884-898, 2013.

Hebbeln, D., Marchant, M., Freudenthal, T., Wefer, G.: Surface distribution along the Chilean continental slope related to upwelling and productivity. Marine Geology 164, 119–137, 2000.

Hebbeln, D., Marchant, M. and Wefer, G.: Paleoproductivity in the southern Peru ^ Chile Current through the last 33 000 yr, Mar. Geol., 186, 2002.

Helly, J. and Levin. L.: Global distribution of naturally occurring marine hypoxia on continental margin, Deep-Sea Res. Pt. I, 51, 1159-1168, 2004.

Heusser, C. J. and Moar, N. T.: Pollen and spores of chile: Modern types of the pteridophyta, gymnospermae, and angiospermae, New Zeal. J. Bot., 11(2), 389–391, doi:10.1080/0028825X.1973.10430287, 1973.

Huerta-Diaz, M. A. and Morse, J. W.: Pyritization of trace metals in anoxic marine sediments, Geochim. Cosmochim. Acta, 56(7), 2681–2702, doi:10.1016/0016-7037(92)90353-K, 1992.

Iriarte, J.L. and González, H.: Phytoplankton size structure during and after the 1997/98 El Niño in a coastal upwelling area of the northern Humboldt Current System, Mar. Ecol. Prog. Ser., 269, 83 – 90, 2004.

Jenny, B., Wilhelm, D., Valero-Garcés, B.L.: The Southern Westerlies in Central Chile: Holocene precipitation estimates based on a water balance model for Laguna Aculeo (33°50’S), Clim. Dynam., 20, 269–280, DOI 10.1007/s00382-002-0267-3, 2003.

Kaiser, J., Schefuß, E., Lamy, F., Mohtadi, M., Hebbeln, D.:Glacial to Holocene changes in sea surface temperature and coastal vegetation in north central Chile: high versus low latitude forcing, Quat. Sci. Rev., 27, 2064–2075, 2008.

Keshav, N. and Achyuthan, H.: Late Holocene continental shelf sediments, off Cuddalore, East coast, Bay of Bengal, India: Geochemical implications for source-area weathering and provenance, Quat. Int., 371, 209–218, doi:10.1016/j.quaint.2015.03.002, 2015.

Klinkhammer, G. P. and Palmer, M. R. Uranium in the oceans: Where it goes and why, Geochim. Cosmochim. Ac., 55(7), 1799–1806, doi: 10.1016/0016-037(91)90024-Y, 1991.

Koutavas, A., deMenocal, P.B., Olive, G.C., Lynch-Stieglitz, J.: Mid-Holocene El Niño–Southern Oscillation (ENSO) attenuation revealed by individual foraminifera in eastern tropical Pacific sediments, 34(12), 993–996, doi: 10.1130/G22810A, 2006.

Lambeck, K., Rouby, H., Purcella, A., Sunc, Y., Sambridge, M.: Sea level and global ice volumes from the Last Glacial Maximum to the Holocene, PNAS, 111(43), 15296-15303, 2014.

Lamy F., Hebbeln, D., Wefer, G.: High-Resolution Marine Record of Climatic Change in Mid-latitude Chile during the Last 28,000 Years Based on Terrigenous Sediment Parameters, Quat. Res., 51**,** 83–93, 1999.

Lamy, F., Hebbeln, D., Röhl, U. and Wefer, G.: Holocene rainfall variability in southern Chile: a marine record of latitudinal shifts of the Southern Westerlies. Earth Planet. Sc. Lett., 185, 369–382, 2001.

Lamy, F., Rühlemann, C., Hebbeln, D. and Wefer, G.: High- and low-latitude climate control on the position of the southern Peru-Chile Current during the Holocene, Paleoceanography, 17(2), 16-1-16–10, doi:10.1029/2001PA000727, 2002.

Lamy, F., Kilian, R., Arz, H.W., Francois J-P., Kaiser, J.,Prange, M. and Steinke, T.: Holocene changes in the position and intensity of the southern westerly wind belt, Nat. Geosci., 3, 695–699, 2010.

Little, S. H., Vance, D., Walker-Brown, C. and Landing, W. M.: The oceanic mass balance of copper and zinc isotopes, investigated by analysis of their inputs, and outputs to ferromanganese oxide sediments, Geochim. Cosmochim. Acta, 125, 673–693, doi:10.1016/j.gca.2013.07.046, 2014.

Maldonado, A., Villagrán, C.,:Paleoenvironmental changes in the semiarid coast of Chile (~32°S) during the last 6200 cal years inferred from a swamp-forest pollen record. Quat. Res., 58, 130–138, 2002.

Maldonado, A. and Rozas, E.: Clima y Paleoambientes durante el Cuaternario Tardío en la Región de Atacama, in Libro Rojo de la Flora Nativa y de los Sitios Prioritarios para su Conservación: Región de Atacama, pp. 293–304., 2008.

Maldonado, A. and Villagrán, C.: Climate variability over the last 9900 cal yr BP from a swamp forest pollen record along the semiarid coast of Chile, Quat. Res., 66(2), 246–258, doi:10.1016/j.yqres.2006.04.003, 2006.

Marchant, M., Hebbeln, D. and Wefer, G.: High resolution foraminiferal record of the last 13,300 yeras from the upwelling area off Chile, Mar. Geol., 161, 115–128, doi:https://doi.org/10.1016/S0025-3227(99)00041-9, 1999.

Mazzullo, J., Gilbert, A., Rabinowitz, P., Meyer, A. and Garrison, L.: Handbook for Shipboard Sedimentologists, 67 pp., 1988.

Mohtadi, M., Rossel, P., Lange, C.B., Pantoja, S., Böning, P., Repeta, D., Grunwald, M., Lamy, F., Hebbeln, D., Brumsack, H-J.: Deglacial pattern of circulation and marine productivity in the upwelling region off central-south Chile, Earth Planet. Sci. Lett. , 272, 221–230, 2008.

Montecinos, A., and Aceituno, P.: Seasonality of the ENSO-Related Rainfall Variability in Central Chile and Associated Circulation Anomalies. J. Climate., 16, 281–296, 2003.

Montecinos, S., Gutiérrez, J. R., López-Cortés, F. and López, D.: Climatic characteristics of the semi-arid Coquimbo Region in Chile, J. Arid Environ., 126, 7–11, doi:10.1016/j.jaridenv.2015.09.018, 2016.

Moraga-Opazo, J., Valle-Levinson, A., Ramos, M. and Pizarro-Koch, M.: Upwelling-Triggered near-geostrophic recirculation in an equatorward facing embayment, Cont. Shelf Res., 31, 1991–1999, 2011.

Mortlock, R. A. and Froelich, P. N.: A simple method for the rapid determination of biogenic opal in pelagic marine sediments, Deep Sea Res. Part A, Oceanogr. Res. Pap., 36(9), 1415–1426, doi:10.1016/0198-0149(89)90092-7, 1989.

Morse, J.W. and Luther, G.W.: Chemical influences on trace metal–sulfide interactions in anoxic sediments. Geochim Cosmochim Ac., 63, 3373–3378, 1999.

Moy, C.M., Seltzer, G.O., Rodbell, D.T. and Anderson, D.M.: Variability of El Niño/Southern Oscillation activity at millennial timescales during the Holocene epoch. Nature, 420(6912), p.162, 2002.

Muñoz, P., Dezileau, L., Dezileau, L., Lange, C.B., Cardenas, L., Sellanes, J., Salamanca, M.A., Maldonado, A.: Evaluation of sediment trace metal records as paleoproductivity and paleoxygenation proxies in the upwelling center off Concepción, Chile (36°S)., Prog. Oceanogr., 92–95, 66–80, 2012.

Nakanishi, T. and Minagawa, M.: Stable carbon and nitrogen isotopic compositions of sinking particles in the northeast Japan Sea, Geochem. J., 37(2), 261–275, doi:https://doi.org/10.2343/geochemj.37.261, 2003.

Nameroff, T., Balistrieri, L. and Murray, W.: Suboxic trace metals geochemistry in the eastern tropical North Pacific, Geochim Cosmochim Ac., 66(7), 1139–1158, 2002.

Ogrinc, N., Fontolan, G., Faganeli, J. and Covelli, S.: Carbon and nitrogen isotope compositions of organic matter in coastal marine sediments (the Gulf of Trieste, N Adriatic Sea): indicators of sources and preservation, Mar. Chem., 95, 163-181, 2005.

Ohnemus, D. C. and Lam, P. J.: Cycling of lithogenic marine particles in the US GEOTRACES North Atlantic transect, Deep. Res. Part II Top. Stud. Oceanogr., 116, 283–302, doi:10.1016/j.dsr2.2014.11.019, 2015.

Ortega, C., Vargas, G., Rutllant, J.A., Jackson, D., Méndez, C.: Major hydrological regime change along the semiarid western coast of South America during the early Holocene, Quaternary Res., 78, 513-527, http://dx.doi.org/10.1016/j.yqres.2012.08.002, 2012.

Ota, Y. and Paskoff, R.: Holocene deposits on the coast of north-central Chile: radiocarbon ages and implications for coastal changes. Rev. Geol. Chile, 20, 25−32, 1993.

Paytan, A.: Ocean paleoproductivity, Encyclopedia of Paleoclimatology and Ancient Environments, Encyclopedia of Earth Science Series, Gornitz, V. (Ed.), Kluwer Academic Publishers. 2008.

Peacock, C.L. and Sherman, D.M.: Copper(II) sorption onto goethite, hematite and lepidocrocite: a surface complexation model based on ab initio molecular geometries and EXAFS spectroscopy. Geochim. Cosmochim. Ac., 68, 2623–2637, 2004.

Pizarro, O., Shaffer, G., Dewitte, B. and Ramos, M.: Dynamics of seasonal and interannual variability of the Peru-Chile Undercurrent, Geophys. Res. Lett., 29(12), 28–31, doi:10.1029/2002GL014790, 2002.

Quintana, J.M. and Aceituno, P.: Changes in the rainfall regime along the extratropical west coast of South America (Chile): 30-43º S, Atmosfera, 25(1), 1 – 22, 2012.

Ramos, M., Pizarro,O., Bravo, L. and Dewitte, B.: Seasonal variability of the permanent thermocline off northern Chile, Geophys. Res. Lett., 33, L09608, doi:10.1029/2006GL025882, 2006.

Ramos, M., Dewitte, B., Pizarro, O. and Garric, G.: Vertical propagation of extratropical Rossby waves during the 1997–1998 El Niño off the west coast of South America in a medium-resolution OGCM simulation, J. Geophys. Res., 113, C08041, doi:10.1029/2007JC004681, 2008.

Rau, H. G., Takahashi, T. and Des Marais, D. J.: Latitudinal variations in plankton δ13C: implications for CO2 and productivity in past oceans, Nature, 341, 516–518, 1989.

Reimer, P. J., Bard, E., Bayliss, A., Beck, J. W., Blackwell, P. G., Ramsey, C. B., Buck, C. E., Cheng, H., Edwards, R. L., Friedrich, M., Grootes, P. M., Guilderson, T. P., Haflidason, H., Hajdas, I., Hatté, C., Heaton, T. J., Hoffmann, D. L., Hogg, A. G., Hughen, K. A., Kaiser, K. F., Kromer, B., Manning, S. W., Niu, M., Reimer, R. W., Richards, D. A., Scott, E. M., Southon, J. R., Staff, R. A., Turney, C. S. M. and van der Plicht, J.: IntCal13 and Marine13 Radiocarbon Age Calibration Curves 0–50,000 Years cal BP, Radiocarbon, 55(4), 1869–1887, doi:10.2458/azu_js_rc.55.16947, 2013.

Rein, B., Lückge, A., Reinhardt, L., Sirocko, F., Wolf, A., Dullo, W-C.: El Niño variability off Peru during the last 20,000 years, Paleoceanogr., PA4003, doi:10.1029/2004PA001099, 2005

Rodbell, D.T., Seltzer, G.O., Anderson, D.M., Abbott, M.B, Enfield, D.B, Newman JH: An approximately 15,000-year record of El Nino-driven alluviation in southwestern Ecuador, Science, 283, 516 – 520, 1999.

Romero, O., Kim, J-H, Hebbeln, D.: Paleoproductivity evolution off central Chile from the Last Glacial Maximum to the Early Holocene, Quat. Res., 65, 519 – 525, 2006.

Saavedra-Pellitero,M., Flores, J. A., Lamy, F., Sierro, F. J., Cortina, A.: Coccolithophore estimates of paleotemperature and paleoproductivity changes in the southeast Pacific over the past ∼27 kyr.

Sabatier, P., Dezileau, L., Blanchemanche, P., Siani, G., Condomines, M., Bentaleb, I. and Piquès, G.: Holocene variations of radiocarbon reservoir ages in a mediterranean lagoonal system, Radiocarbon, 52(1), 91–102, doi:10.1017/S0033822200045057, 2010.

Saito, C., Noriki, S. and Tsunogai, S.: Particulate flux of Ai, a component of land origin, in the western North Pacific, Deep-Sea Res., 39, 1315–1327, 1992.

Salvatteci, R., Gutiérrez, D., Field, D., Sifeddine, A., Ortlieb, L., Bouloubassi, I., Boussafir, M., Boucher, H. and Cetin, F.: The response of the Peruvian Upwelling Ecosystem to centennial-scale global change during the last two millennia, Clim. Past, 10(2), 715–731, doi:10.5194/cp-10-715-2014, 2014.

Schrader H. J. and Gersonde, R.: Diatoms and silicoflagellates. Utrecht Micropaleontol. Bull. 17, 129–176, 1978.

Sellanes, J., Quiroga, E., Neira, C., Gutiérrez, D., : Changes of macrobenthos composition under different ENSO cycle conditions on the continental shelf off central Chile, Cont. Shelf. Res. 27, 1002 –1016, 2007.

Shaffer, G., Pizarro, O. Djurfeldt, L., Salinas, S. and Rutllant, J.: Circulation and low-frequency variability near the Chilean coast: Remotely forced fluctuations during the 1991– 92 El Niño, J. Phys. Oceanogr., 27, 217– 235, 1997.

Sigman, D.M., Karsh, K.L., Casciotti, K.L.: Ocean process tracers: nitrogen isotopes in the ocean. Encyclopedia of ocean science, 2nd edn Elsevier, Amsterdam.
Sims, P.A. 1996. An Atlas of British Diatoms. Biopress Ltd, Bristol United Kingdom 601, 2009.

Sun, X., Higgins, J. and Turchyn, A. V.: Diffusive cation fluxes in deep-sea sediments and insight into the global geochemical cycles of calcium, magnesium, sodium and potassium, Mar. Geol., 373, 64–77, doi:10.1016/j.margeo.2015.12.011, 2016.

Sundby, B., Martinez, P. and Gobeil, C.: Comparative geochemistry of cadmium, rhenium, uranium, and molybdenum in continental margin sediments, Geochim. Cosmochim. Ac., 68, 2485–2493, 2004.

Sweeney, R. E., Kaplan I. R.: Natural abundances of 15N as a source indicator of nearshore marine sedimentary and dissolved nitrogen, Mar. Chem., 9, 81− 94, 1980.

Thomas, C. D., Bodsworth, E. J., Wilson, R. J., Simmons, A. D., Davies, Z. G., Musche, M. and Conradt, L.: Ecological and evolutionary processes at expanding range margins, Nature, 411, 577−581, 2001.

Torres, M. E., Brumsack, H. J., Bohrman, G. and Emeis, K. C.: Barite front in continental margin sediments: a new look at barium remobilization in the zone of sulfate reduction and formation of heavy barites in diagenetic fronts, Chem. Geol., 127, 125–139, 1996.

Torres, R., and Ampuero, P.: Strong CO2 outgassing from high nutrient low chlorophyll coastal waters off central Chile (30°S): The role of dissolved iron, Estuar. Coast. Shelf S., 83, 126−132, doi:10.1016/j.ecss.2009.02.030, 2009.

Tribovillard, N., Algeo, T. J., Lyons, T. and Riboulleau, A.: Trace metals as paleoredox and paleoproductivity proxies: an update. Chem. Geol., 232, 12–32, 2006.

Vance, D., Archer, C., Bermin, J., Perkins, J., Statham, P. J., Lohan, M. C., Ellwood, M. J. and Mills, R. A.: The copper isotope geochemistry of rivers and the oceans, Earth Planet. Sc. Lett., 274, 204–213, 2008.

Valle-Levinson, A., Moraga, J., Olivares, J. and Blanco, J. L.: Tidal and residual circulation in a semi-arid bay: Coquimbo Bay, Chile. Cont. Shelf Res., 20, 2009–2018, 2000.

Valle-Levinson, A. and Moraga-Opazo, J.: Observations of bipolar residual circulation in two equatorward-facing semiarid bays, Cont. Shelf Res., 26(2), 179–193, doi:10.1016/j.csr.2005.10.002, 2006.

Van der Weijden, C.: Pitfalls of normalization of marine geochemical data using a common divisor, Mar. Geol., 184, 167–187, 2002.

Vargas, G., Ortlieb, L., Pichon, J. J., Bertaux, J. and Pujos, M.: Sedimentary facies and high resolution primary production inferences from laminated diatomacous sediments off northern Chile (23°S), Mar. Geol., 211(1–2), 79–99, doi:10.1016/j.margeo.2004.05.032, 2004.

Vargas, G., Rutllant, J., Ortlieb, L.: ENSO tropical–extratropical climate teleconnections and mechanisms for Holocene debris flows along the hyperarid coast of western South America (17°–24°S), Earth Planet. Sci. Lett., 249, 467–483, 2006.

Vargas, G., Pantoja, S., Rutllant, J., Lange, C. and Ortlieb, L.: Enhancement of coastal upwelling and interdecadal ENSO-like variability in the Peru-Chile Current since late 19th century. Geophys. Res. Lett., 34, L13607, 2007.

Veit, H.: Southern Westerlies during the Holocene deduced from geomorphological and pedological studies in the Norte Chico, Northern Chile (27–33°S). *Palaeogeogr., Palaeoclimatol., Palaeoecol.,* 123**,** 107–119, 1996.

Williams, P. M. and Gordon, L. I.: Carbon-13:carbon-12 ratios in dissolved and particulate organic matter in the sea. Deep-Sea Res., 17, 19–27, 1970.

Xu, G., Liu, J., Pei, S., Kong, X., Hu, G. and Gao, M.: Source identification of aluminum in surface sediments of the Yellow Sea off the Shandong Peninsula, Acta Oceanol. Sin., 34(12), 147–153, doi:10.1007/s13131-015-0766-9, 2015.

Zheng, Y., Anderson, R. F., van Geen, A. and Fleisheir, M.Q.: Preservation of non-lithogenic particulate uranium in marine sediments. Geochim. Cosmochim. Ac., 66, 3085–3092, 2002.

Acknowledgments

We would like to thank the R/V Stella Maris II crew of Universidad Católica del Norte for their help and support during field work. We extend our acknowledgements to the laboratory assistants of the Paleoceanography Lab at Universidad de Concepción, for their aid in sample analyses. We also wish to thank Dr. Olivier Bruguier of CNRS and his lab personnel for their assistance during ICPMs analyses. We also express our gratitude to INNOVA 07CN13 IXM-150. This manuscript was funded by FONDECYT Project No. 1140851. Partial support from the COPAS Sur-Austral (CONICYT PIA PFB31) and FONDAP-IDEAL centers (No. 15150003) is also acknowledged.

Tables

Table 1. Concentration of elements in Pachingo wetland sediments, considered as lithogenic background for the study area. The values correspond to mean concentrations in surface sediments (0–3 cm).

Element	Metal/Al x 10^3	S
Ca	686.5	139.3
Fe	591.3	84.5
P	8.6	0.7
Sr	5.7	0.6
Ba	5.6	0.1
Cu	0.258	0.019
Ni	0.174	0.005
U	0.020	0.003
Mo	0.020	0.003
Cd	0.0021	0.0003
Re	0.00004	0.00001

Table 2. Radiocarbon dates for BGGC5 and BTGC8 sediment cores collected from mixed planktonic foraminifera and monospecific benthic foraminifera (*Bolivina plicata*), respectively. The ^{14}C-AMS was performed at NOSAM-WHOI. The lab code and conventional ages collected from each core section is indicated. For error calculations see http://www.whoi.edu/nosams/radiocarbon-data-calculations.

Core identification	material	mass (mg)	Lab Code NOSAM	Modern fraction pMC	1σ error	Conventional Age BP	1σ error
BGGC5	Planktonic foraminifera						
10-11	mix	1,8	OS-122160	0,8895	0,0027	940	25
18-19	mix	1,1	OS-122141	0,7217	0,0024	2.620	25
31-32	mix	2,7	OS-122161	0,6590	0,0021	3.350	25
45-46	mix	2	OS-122162	0,6102	0,0017	3.970	25
55-56	mix	1,6	OS-122138	0,5864	0,0025	4.290	35
66-67	mix	2,8	OS-122304	0,5597	0,0018	4.660	25
76-77	mix	2,6	OS-122163	0,4520	0,0016	6.380	30
96-97	mix	1,1	OS-122139	0,4333	0,0033	6.720	60
115-116	mix	4,7	OS-122164	0,3843	0,0016	7.680	35
BTGC8	Benthic foraminifera						
5-6	Bolivina plicata	4,2	OS-130657	0,8953	0,0017	890	15
20-21	Bolivina plicata	7,7	OS-123670	0,7337	0,0021	2.490	25
30-31	Bolivina plicata	13	OS-123671	0,6771	0,0016	3.130	20
40-41	Bolivina plicata	11	OS-123672	0,6507	0,0019	3.450	25
50-51	Bolivina plicata	8,7	OS-123673	0,5877	0,0014	4.270	20
60-61	Bolivina plicata	13	OS-123674	0,5560	0,0018	4.720	25
71-72	Bolivina plicata	10	OS-123675	0,4930	0,0013	5.680	20
80-81	Bolivina plicata	7,3	OS-123676	0,4542	0,0012	6.340	20
90-91	Bolivina plicata	6,8	OS-123677	0,4259	0,0015	6.860	30
96-97	Bolivina plicata	6,8	OS-123678	0,3903	0,0013	7.560	25

Table 3. Reservoir age (DR) estimation considering the ^{210}Pb age determined with the CRS model (McCaffrey and Thomson, 1980) at a selected depth sections of the core, compared with ^{14}C ages (yr BP) from marine13.14 curve (Reimer et al., 2013), according to Sabatier et al. (2010).

Core	Depth (cm)	Age from CRS model (AD)[a]	Age years BP[b]	^{14}C age Marine 13.14	^{14}C age BP from foram.	DR
BGGC5	10.5	1828	122	499±24	940±25	441±35
BTCG8	5.5	1908	42	448±23	890±15	442±27

[a]Anno Domini
[b]Before present=1950

Table 4. Spearman rank order correlations for geochemical data. Significant values >0.8 are indicated in bold.

BGGC5

	Al	P	K	Ca	Mn	Fe	Ni	Cu	Mo	Cd	Re	Sr	U	Ba	Opal	TOC
Al	1.00	-0.62	0.49	-0.48	0.64	0.60	-0.75	0.56	-0.10	-0.73	-0.08	-0.33	0.08	0.49	-0.52	-0.44
P		1.00	-0.31	0.37	-0.45	-0.56	0.56	-0.57	0.01	0.61	-0.11	0.39	-0.12	-0.20	0.49	0.24
K			1.00	-0.24	**0.90**	**0.83**	-0.29	0.47	0.28	-0.42	0.33	-0.12	0.50	0.26	-0.25	-0.19
Ca				1.00	-0.47	-0.50	0.44	-0.64	0.23	0.59	0.39	**0.92**	0.30	-0.60	0.18	0.32
Mn					1.00	**0.94**	-0.51	0.68	-0.01	-0.68	0.07	-0.32	0.24	0.43	-0.39	-0.31
Fe						1.00	-0.49	**0.81**	0.03	-0.70	0.11	-0.40	0.23	0.36	-0.37	-0.21
Ni							1.00	-0.51	0.49	**0.91**	0.35	0.25	0.26	-0.70	0.72	0.64
Cu								1.00	-0.12	-0.71	-0.06	-0.61	0.00	0.31	-0.39	-0.07
Mo									1.00	0.50	**0.88**	0.10	0.91	-0.48	0.33	0.36
Cd										1.00	0.36	0.42	0.27	-0.67	0.70	0.54
Re											1.00	0.27	**0.92**	-0.50	0.16	0.38
Sr												1.00	0.24	-0.36	0.05	0.17
U													1.00	-0.39	0.10	0.29
Ba														1.00	-0.30	-0.59
Opal															1.00	0.35
TOC																1.00

BTGC8

	Al	P	K	Ca	Mn	Fe	Ni	Cu	Mo	Cd	Re	Sr	U	Ba	Opal	TOC
Al	1.00	-0.19	-0.17	-0.37	-0.02	-0.03	-0.39	-0.04	-0.39	0.02	-0.13	-0.58	-0.19	0.07	-0.41	-0.29
P		1.00	0.23	0.00	0.43	0.28	0.58	0.23	0.37	0.13	-0.04	0.30	0.14	-0.14	0.56	0.13
K			1.00	-0.02	0.54	0.41	0.43	0.22	-0.11	0.05	-0.04	0.19	-0.28	0.28	0.26	0.20
Ca				1.00	-0.33	-0.27	0.00	-0.23	0.39	0.01	0.33	0.50	0.47	-0.34	0.20	0.34
Mn					1.00	0.21	0.64	0.01	0.05	0.33	0.15	0.32	-0.02	0.24	0.32	0.00
Fe						1.00	0.13	0.71	-0.40	-0.48	-0.67	-0.37	-0.62	0.13	0.14	0.10
Ni							1.00	0.24	0.56	0.20	0.25	0.64	0.19	-0.16	**0.80**	0.45
Cu								1.00	-0.25	-0.68	-0.56	-0.22	-0.61	-0.10	0.21	0.37
Mo									1.00	0.45	0.59	0.66	0.69	-0.41	0.58	0.30
Cd										1.00	0.56	0.39	0.52	0.11	0.10	-0.12
Re											1.00	0.53	**0.83**	-0.16	0.13	0.17
Sr												1.00	0.58	-0.13	0.52	0.23
U													1.00	-0.19	0.21	0.00
Ba														1.00	-0.28	-0.42
Opal															1.00	0.39
TOC																1.00

Table 5. Mean authigenic enrichment factor (EF) ± SD of trace elements calculated for Guanaqueros Bay (BGGC5 core). Lithogenic background was estimated from surface sediments of Pachingo wetland cores (see text). Age ranges were based on opal accumulation.

Age range (cal BP)	Diatoms + spicules	Opal (g m^{-2} yr^{-1})	EF_U	EF_{Mo}	EF_{Re}	EF_{Fe}	EF_{Mn}	EF_{Ba}	EF_{Cd}	EF_{Ni}	EF_{Cu}	EF_P
-65 – 260	lower	30 ±15	2.6 ±0.7	5.5 ±1.3	10.5 ±2.0	0.8 ±0.1	0.5 ±0.1	0.8 ±0.1	30.4 ±6.3	1.4 ±0.2	3.6 ±1.3	2.0 ±0.4
260 – 2100	lower	3 ±2	5.9 ±1.1	15.0 ±2.7	18.4 ±2.8	0.9 ±0.1	0.5 ±0.1	0.8 ±0.1	44-9 ±6.8	1.9 ±0.1	2.9 ±0.3	2.2 ±0.4
2100 – 4600	moderated	12 ±5	5.4 ±0.5	14.4 ±1.5	19.9 ±2.0	0.9 ±0.1	0.5 ±0.1	0.8 ±0.1	55.6 ±12-8	2.4 ±0.2	3.2 ±0.5	2.2 ±0.3
4600 – 6500	higher	4 ±1	5.2 ±0.9	16.9 ±4.1	19.7 ±3.7	0.9 ±0.1	0.5 ±0.1	0.8 ±0.1	127.0 ±46.7	3.3 ±0.5	3.2 ±0.4	3.0 ±0.1
6500 – 8400	higher	32 ±22	4.6 ±0.4	14.3 ±2.6	18.0 ±2.1	0.9 ±0.1	0.5 ±0.1	0.8 ±0.1	146.6 ±25.8	3.4 ±0.4	2.5 ±0.3	3.9 ±0.7

Figures

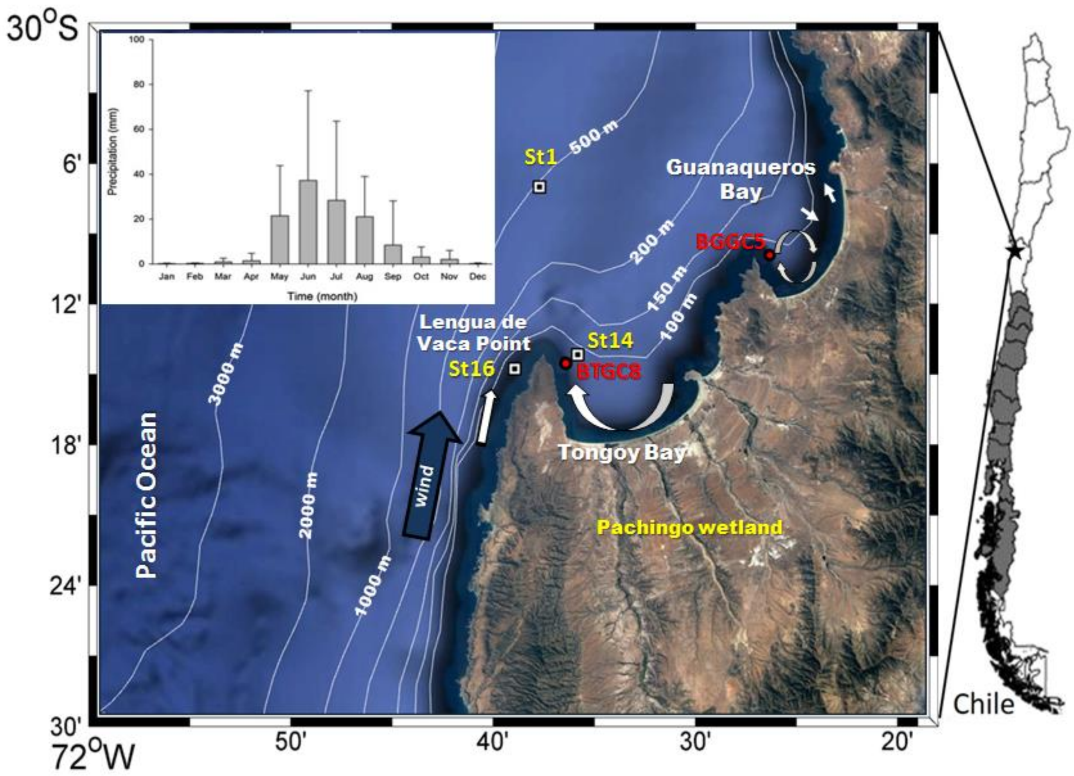

Figure 1. Study area showing the position of sampling stations. Sediment cores were retrieved from Guanaqueros Bay (BGGC5) and from Tongoy Bay (BTGC8) at water depths of 89 and 85 m, respectively. Information of dissolved oxygen (DO) in the water column at ST1and ST16 and of suspended organic particles collected at ST14 sampling sites was gathered in a previous project (INNOVA 07CN13 IXM-150). Monthly precipitation in mm (bars) (means ± SD; Montecinos et al., 2016). Schematic representation of the bays circulation (white arrows) and wind direction is indicated (blue arrow) obtained from Valle-Levinson and Moraga-Opazo (2006) and Moraga-Opazo et al. (2001).

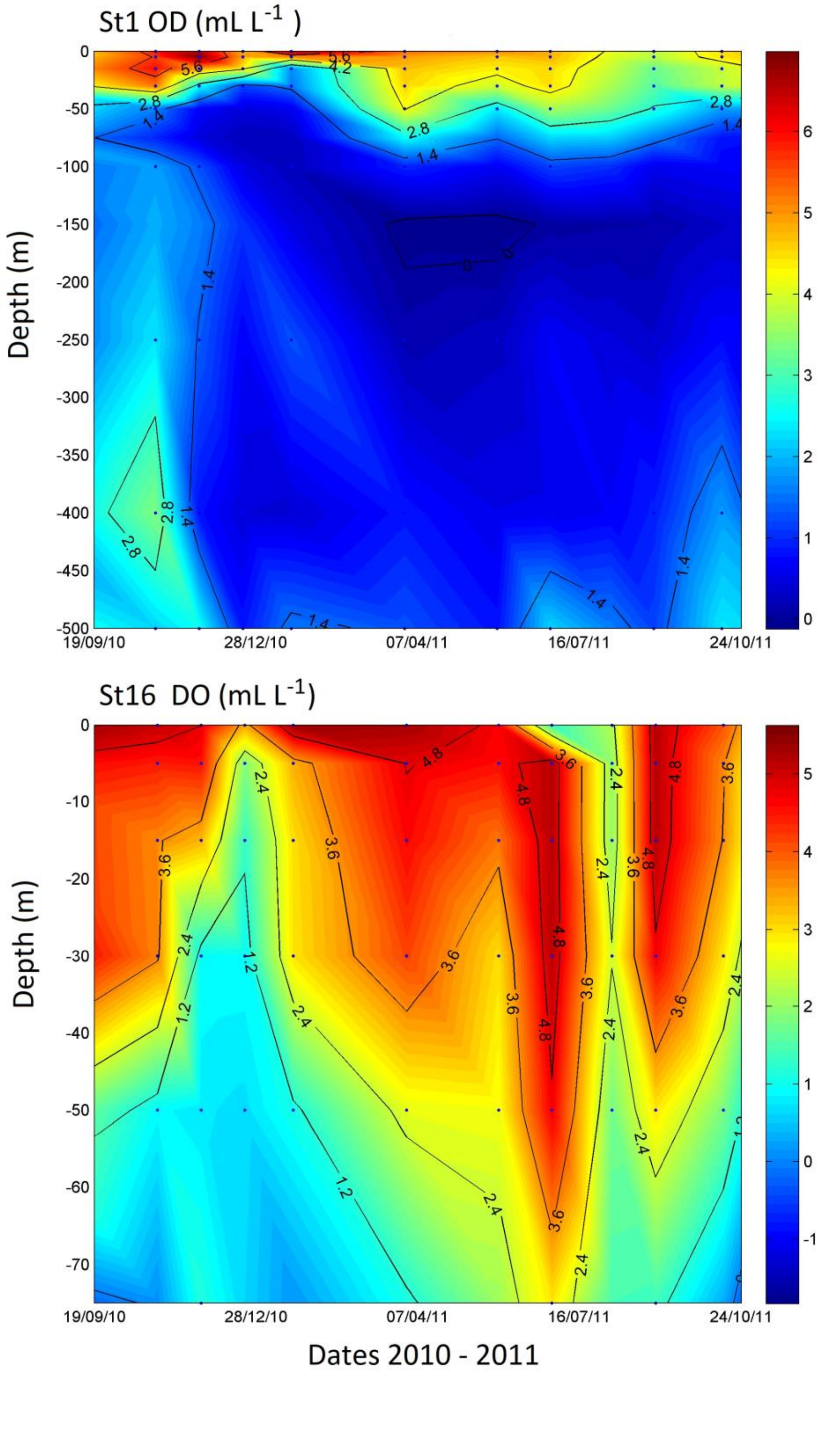

Figure 2. Dissolved Oxygen (DO) time series in the water column measured between October 2010 and January 2011, at stations St1 and St16 off Tongoy Bay, Coquimbo (30°S).

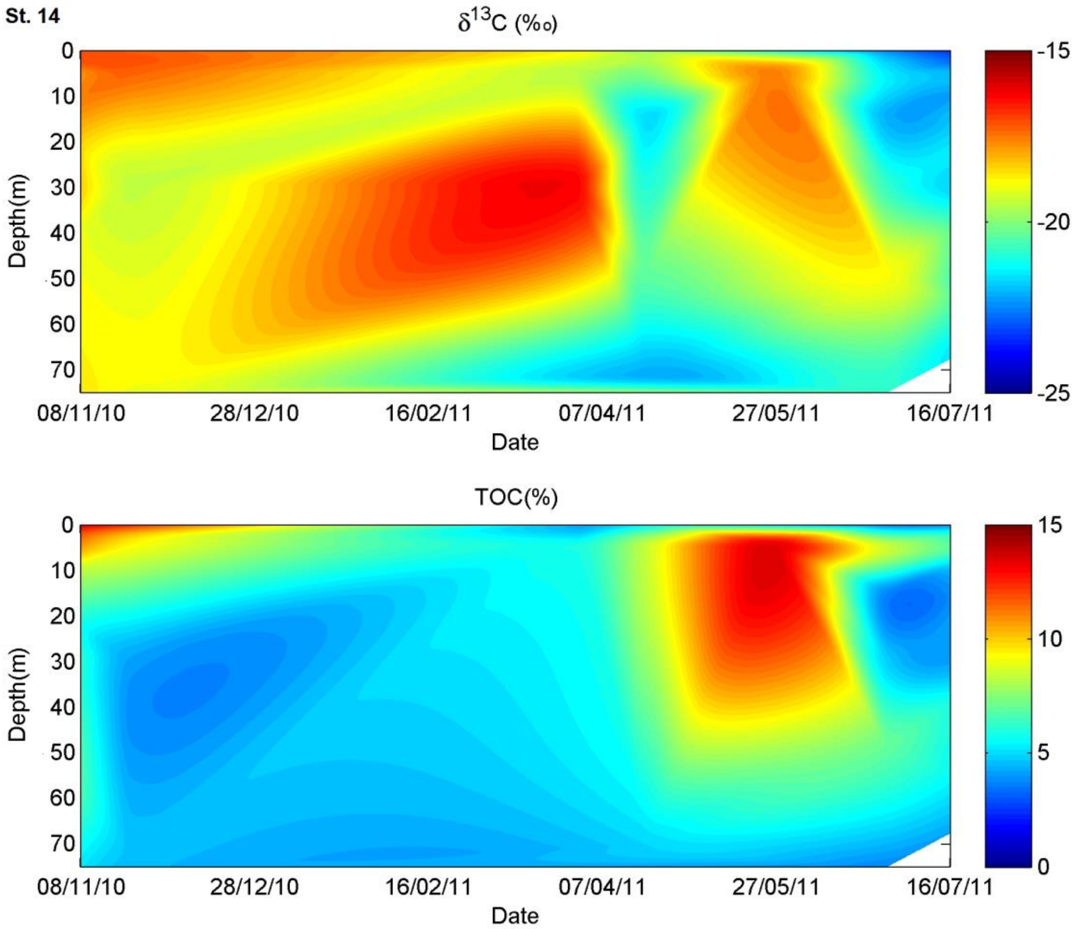

Figure 3. Suspended particulate matter composition (TOC % and δ^{13}Corg) measured in the water column between October 2010 and October 2011, at station St14, Tongoy Bay, Coquimbo (30°S).

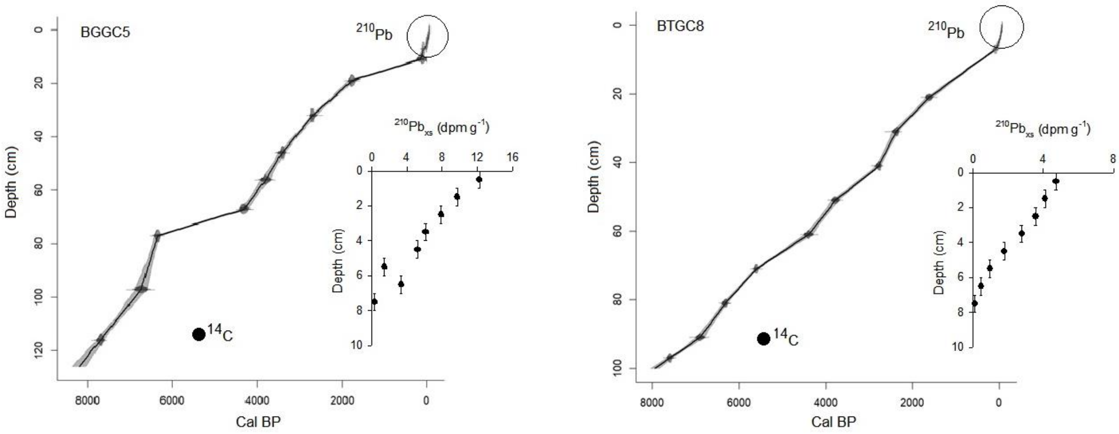

Figure 4. Age model based on ^{14}CAMS and ^{210}Pb measurements. The time scale was obtained according to the best fit of curves of $^{210}Pb_{xs}$ and ^{14}C points using CLAM 2.2 software and Marine curve ^{13}C (Reimer et al., 2013).

a) BGGC5

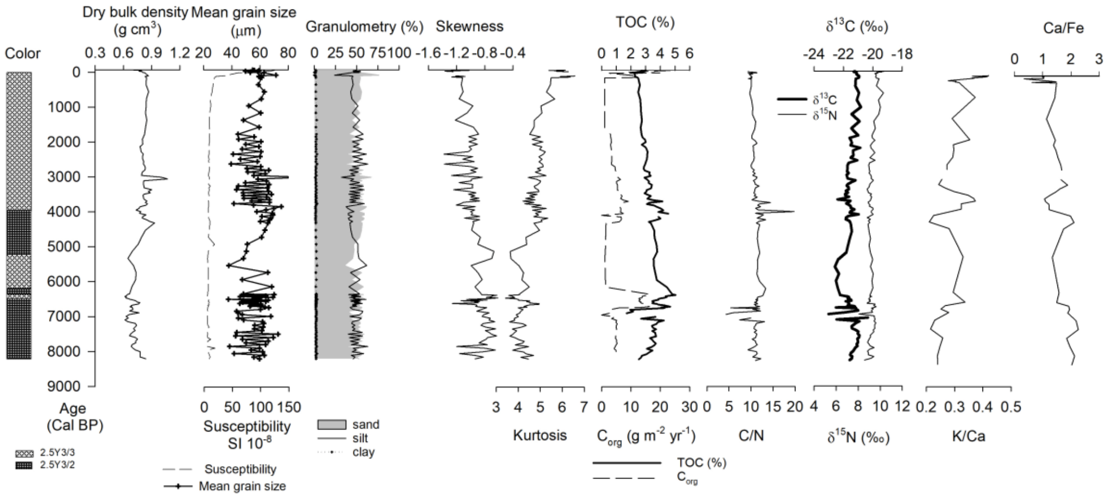

b) BTGC8

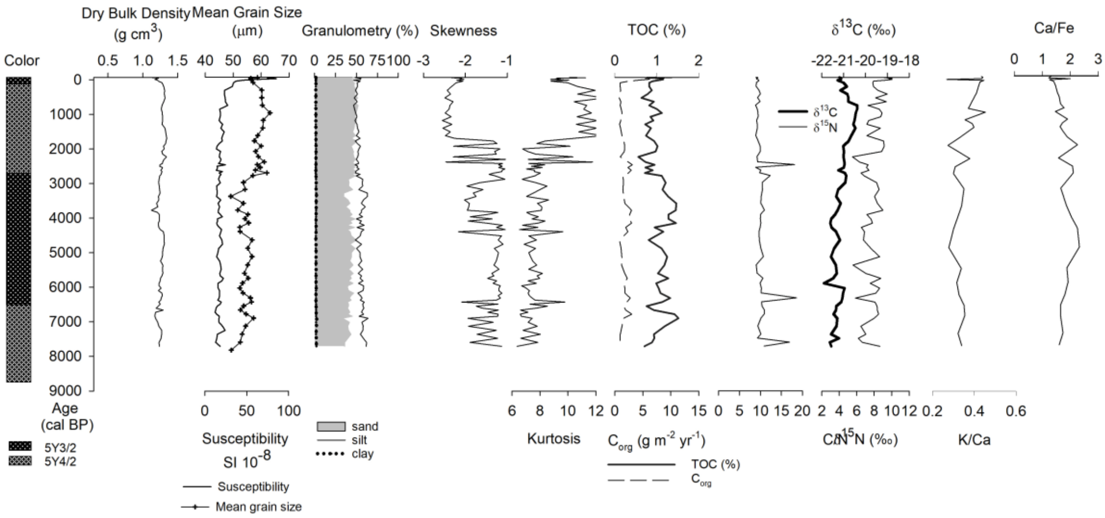

Figure 5. Sediment characterization of sediment cores retrieved from (a) Guanaqueros Bay (BGGC5) and (b) Tongoy Bay (BTGC8). Distribution in depth core of color, dry bulk density, statistical parameters (skewness, mean grain size, kurtosis), organic components (TOC, stable isotopes) and chemical composition (K/Ca, Ca/Fe).

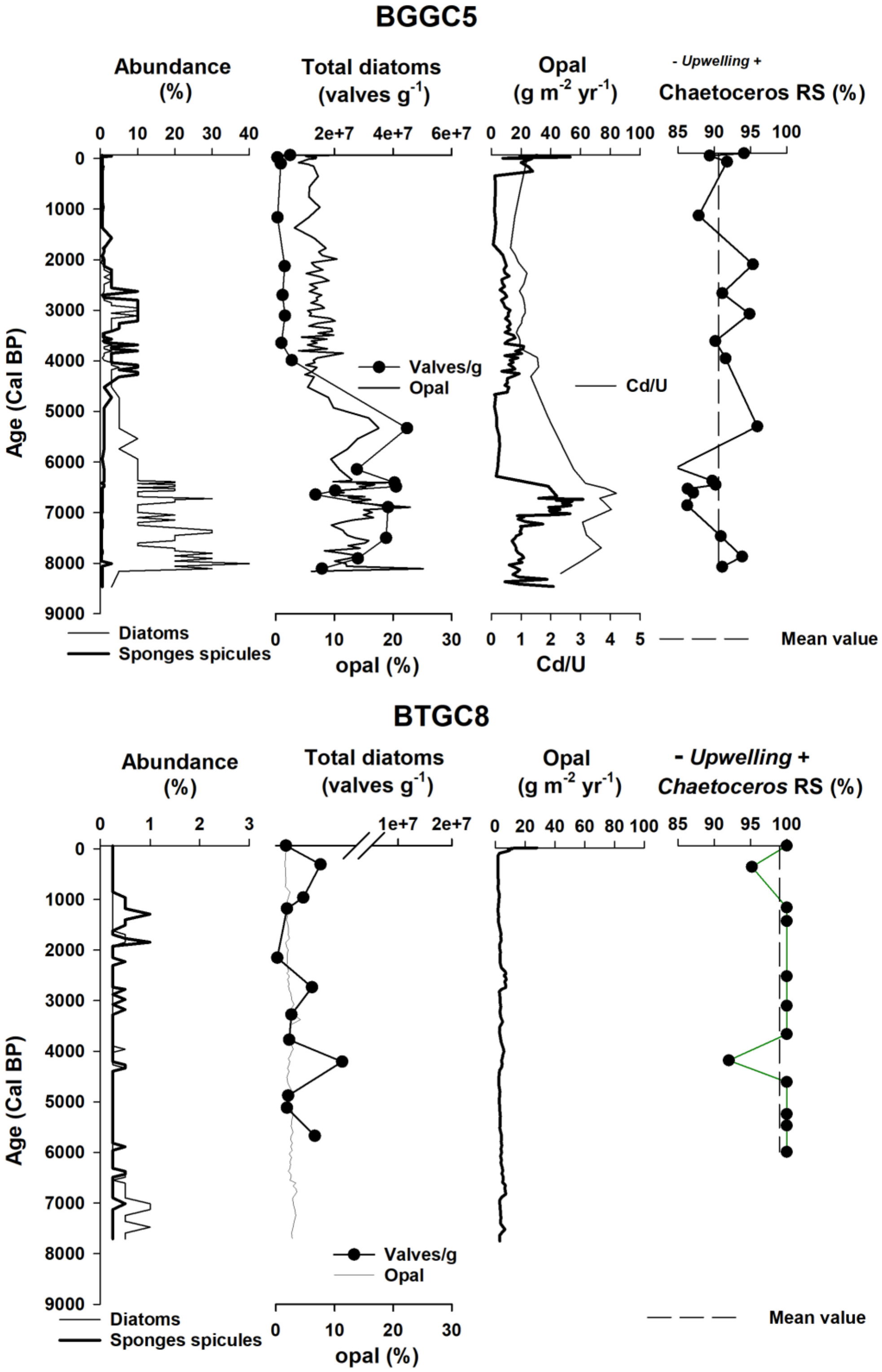

Figure 6. Diatom abundance, opal accumulation and temporal variations in the relative abundance of *Chaetoceros* resting spores in BGGC5 and BTGC8 cores (Guanaqueros and Tongoy Bay, respectively). Cd/U distribution was included as a proxy for redox condition.

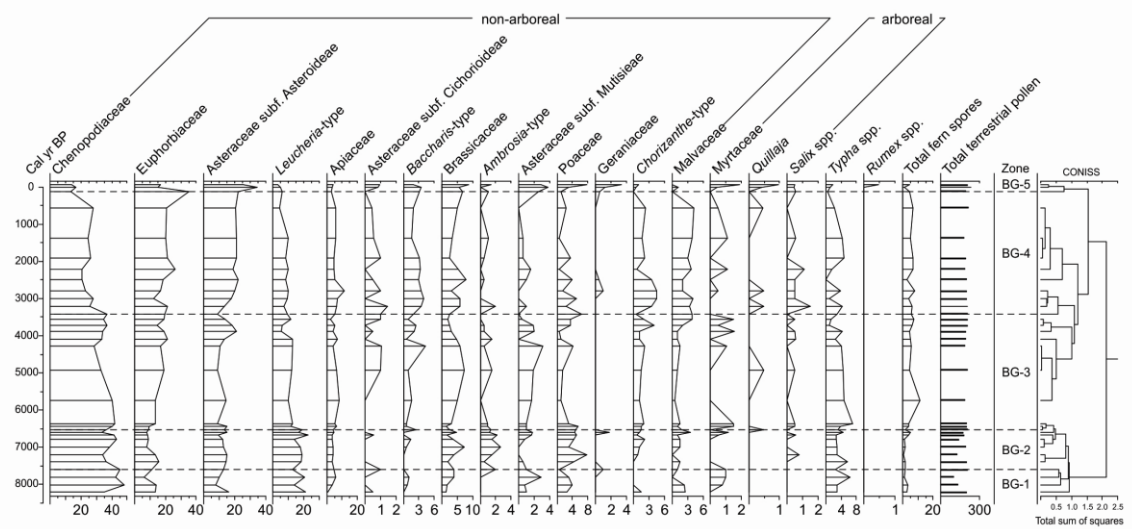

Figure 7. Pollen record in BGGC5 core.

a) BGGC5

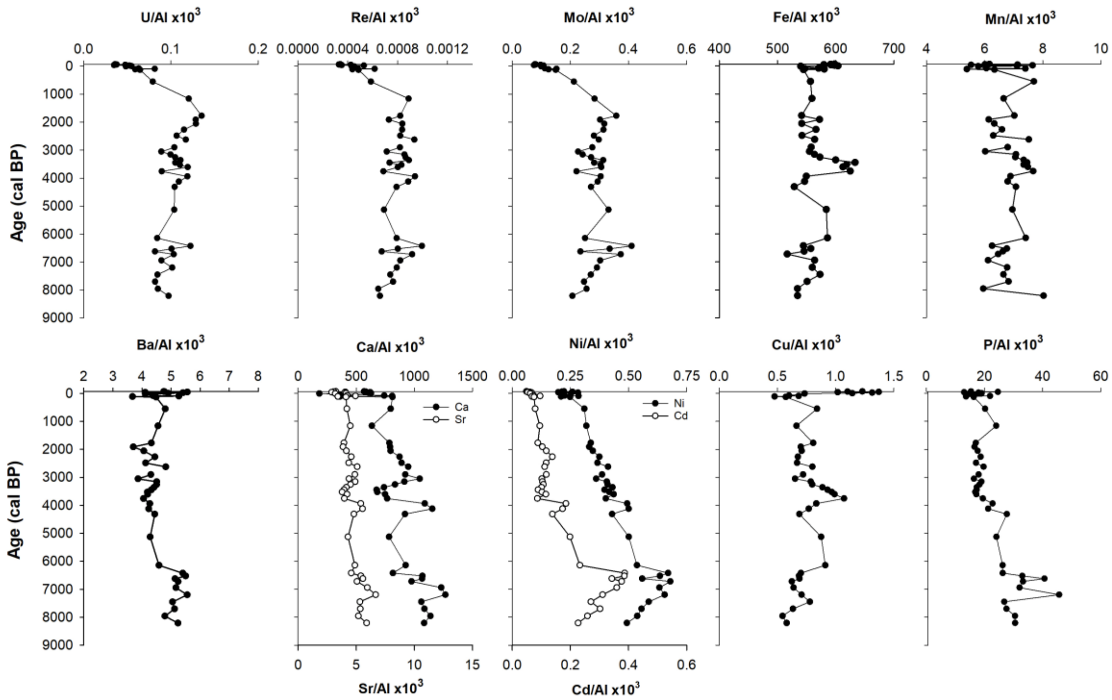

b) BTGC8

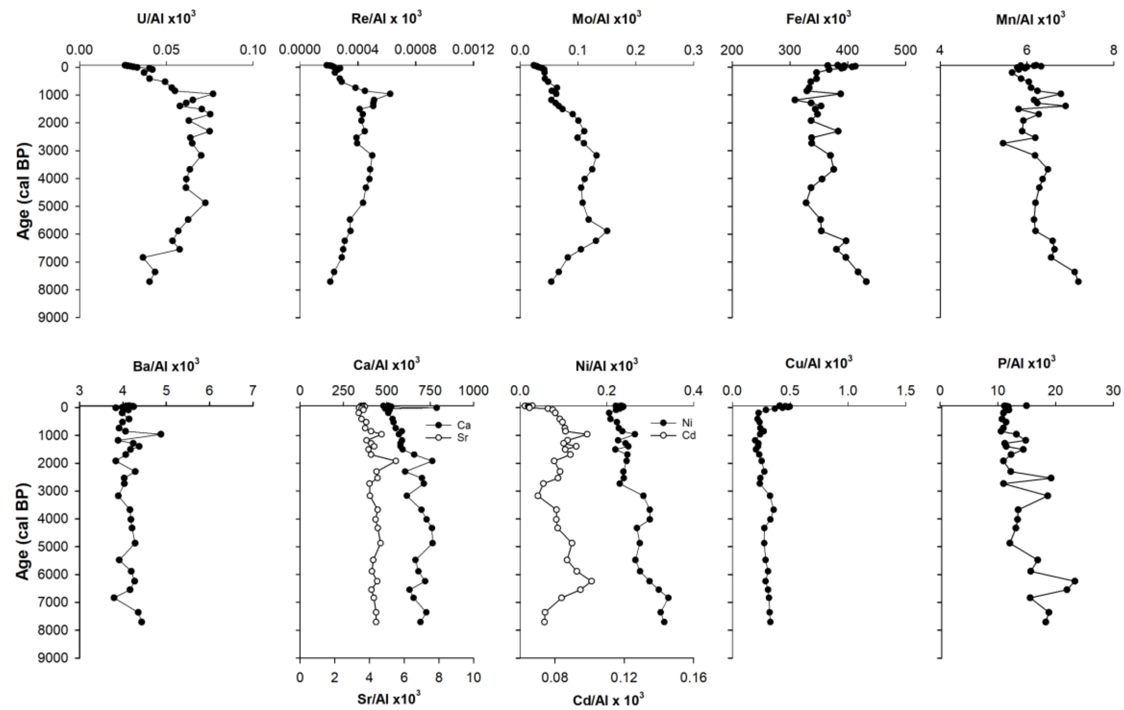

Figure 8. Trace element distribution in sediment cores retrieved from (a) Guanaqueros Bay (BGGC5) and (b) Tongoy Bay (BTGC8), off Coquimbo (30°S).

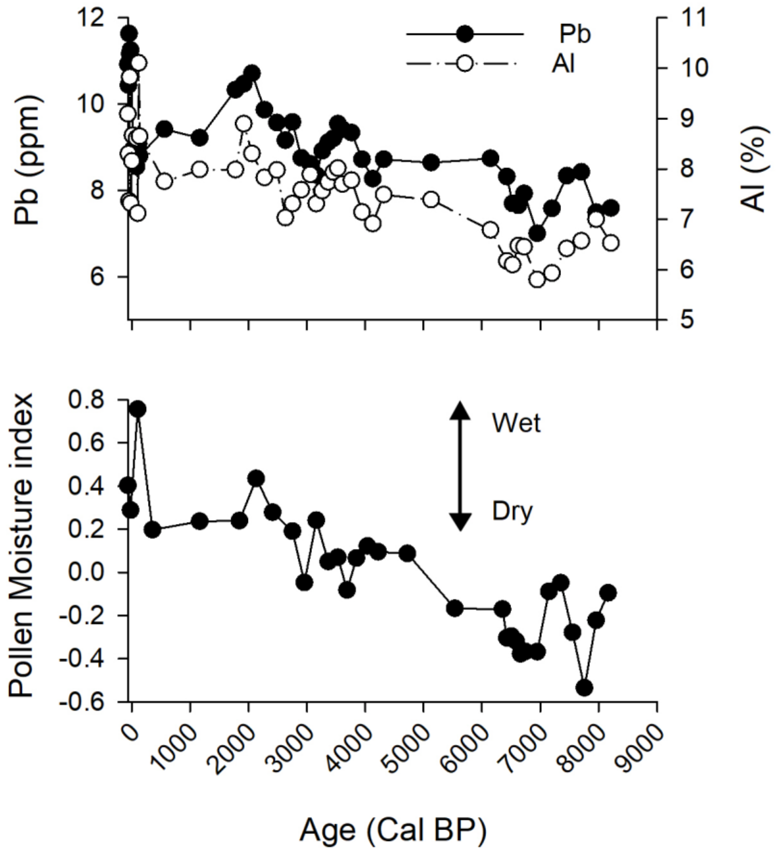

Figure 9. Pollen Moisture Index defined as the normalized ratio between Euphorbiaceae (wet coastal shrub land) and Chenopodiaceae (arid scrubland). Positive (negative) values for this index indicate the relative expansion (reduction) of coastal vegetation under wetter (drier) conditions. Pb and Al distribution at BGGC5 core, representatives of terrigenous input to the bay.